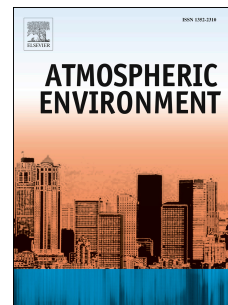


# Accepted Manuscript



Evaluation of operational online-coupled regional air quality models over Europe and North America in the context of AQMEII phase 2. Part II: Particulate Matter

Ulas Im, Roberto Bianconi, Efsio Solazzo, Ioannis Kioutsioukis, Alba Badia, Alessandra Balzarini, Rocío Baró, Roberto Bellasio, Dominik Brunner, Charles Chemel, Gabriele Curci, Hugo Denier van der Gon, Johannes Flemming, Renate Forkel, Lea Giordano, Pedro Jiménez-Guerrero, Marcus Hirtl, Alma Hodzic, Luka Honzak, Oriol Jorba, Christoph Knote, Paul A. Makar, Astrid Manders-Groot, Lucy Neal, Juan L. Pérez, Guidio Pirovano, George Pouliot, Roberto San Jose, Nicholas Savage, Wolfram Schroder, Ranjeet S. Sokhi, Dimiter Syrakov, Alfreida Torian, Paolo Tuccella, Kai Wang, Johannes Werhahn, Ralf Wolke, Rahela Zabkar, Yang Zhang, Junhua Zhang, Christian Hogrefe, Stefano Galmarini

PII: S1352-2310(14)00683-9

DOI: [10.1016/j.atmosenv.2014.08.072](https://doi.org/10.1016/j.atmosenv.2014.08.072)

Reference: AEA 13224

To appear in: *Atmospheric Environment*

Received Date: 30 May 2014

Revised Date: 27 August 2014

Accepted Date: 28 August 2014

Please cite this article as: Im, U., Bianconi, R., Solazzo, E., Kioutsioukis, I., Badia, A., Balzarini, A., Baró, R., Bellasio, R., Brunner, D., Chemel, C., Curci, G., Denier van der Gon, H., Flemming, J., Forkel, R., Giordano, L., Jiménez-Guerrero, P., Hirtl, M., Hodzic, A., Honzak, L., Jorba, O., Knote, C., Makar, P.A., Manders-Groot, A., Neal, L., Pérez, J.L., Pirovano, G., Pouliot, G., San Jose, R., Savage, N., Schroder, W., Sokhi, R.S., Syrakov, D., Torian, A., Tuccella, P., Wang, K., Werhahn, J., Wolke, R., Zabkar, R., , Zhang, Y., Zhang, J., Hogrefe, C., Galmarini, S., Evaluation of operational online-coupled regional air quality models over Europe and North America in the context of AQMEII phase 2. Part II: Particulate Matter, *Atmospheric Environment* (2014), doi: 10.1016/j.atmosenv.2014.08.072.

This is a PDF file of an unedited manuscript that has been accepted for publication. As a service to our customers we are providing this early version of the manuscript. The manuscript will undergo copyediting, typesetting, and review of the resulting proof before it is published in its final form. Please

note that during the production process errors may be discovered which could affect the content, and all legal disclaimers that apply to the journal pertain.

1 **Evaluation of operational online-coupled regional air quality models over**  
 2 **Europe and North America in the context of AQMEII phase 2. Part II:**  
 3 **Particulate Matter**

4

5 Ulas Im<sup>a</sup>, Roberto Bianconi<sup>b</sup>, Efisio Solazzo<sup>a</sup>, Ioannis Kioutsioukis<sup>a</sup>, Alba Badia<sup>c</sup>, Alessandra  
 6 Balzarini<sup>d</sup>, Rocío Baró<sup>e</sup>, Roberto Bellasio<sup>b</sup>, Dominik Brunner<sup>f</sup>, Charles Chemel<sup>g</sup>, Gabriele  
 7 Curci<sup>h</sup>, Hugo Denier van der Gon<sup>i</sup>, Johannes Flemming<sup>j</sup>, Renate Forkel<sup>k</sup>, Lea Giordano<sup>f</sup>,  
 8 Pedro Jiménez-Guerrero<sup>e</sup>, Marcus Hirtl<sup>l</sup>, Alma Hodzic<sup>m</sup>, Luka Honzak<sup>n</sup>, Oriol Jorba<sup>c</sup>,  
 9 Christoph Knote<sup>m</sup>, Paul A. Makar<sup>o</sup>, Astrid Manders-Groot<sup>i</sup>, Lucy Neal<sup>p</sup>, Juan L. Pérez<sup>q</sup>,  
 10 Guidio Pirovano<sup>d</sup>, George Pouliot<sup>r</sup>, Roberto San Jose<sup>q</sup>, Nicholas Savage<sup>p</sup>, Wolfram Schroder<sup>s</sup>,  
 11 Ranjeet S. Sokhi<sup>g</sup>, Dimiter Syrakov<sup>t</sup>, Alfreida Torian<sup>r</sup>, Paolo Tuccella<sup>h</sup>, Kai Wang<sup>u</sup>, Johannes  
 12 Werhahn<sup>k</sup>, Ralf Wolke<sup>s</sup>, Rahela Zabkar<sup>n,v</sup>, Yang Zhang<sup>u</sup>, Junhua Zhang<sup>o</sup>, Christian Hogrefe<sup>r</sup>,  
 13 Stefano Galmarini<sup>a\*</sup>

14

- 15 a. European Commission, Joint Research Centre, Institute for Environment and  
 16 Sustainability, Air and Climate Unit, Ispra (Italy).  
 17 b. Enviroware srl, Concorezzo (MB), Italy.  
 18 c. Earth Sciences Department, Barcelona Supercomputing Center (BSC-CNS),  
 19 Barcelona, Spain.  
 20 d. Ricerca sul Sistema Energetico (RSE SpA), Milano, Italy  
 21 e. University of Murcia, Department of Physics, Physics of the Earth. Campus de  
 22 Espinardo, Ed. CIOyN, 30100 Murcia, Spain.  
 23 f. Laboratory for Air Pollution and Environmental Technology, Empa, Dubendorf,  
 24 Switzerland.  
 25 g. Centre for Atmospheric & Instrumentation Research, University of Hertfordshire,  
 26 College Lane, Hatfield, AL10 9AB, UK.  
 27 h. Department of Physical and Chemical Sciences, Center of Excellence for the forecast  
 28 of Severe Weather (CETEMPS), University of L'Aquila, L'Aquila, Italy.  
 29 i. Netherlands Organization for Applied Scientific Research (TNO), Utrecht, The  
 30 Netherlands.  
 31 j. ECMWF, Shinfield Park, RG2 9AX Reading, United Kingdom.  
 32 k. Karlsruher Institut für Technologie (KIT), Institut für Meteorologie und  
 33 Klimaforschung, Atmosphärische Umweltforschung (IMK-IFU), Kreuzeckbahnstr. 19,  
 34 82467 Garmisch-Partenkirchen, Germany.  
 35 l. Section Environmental Meteorology, Division Customer Service, ZAMG -  
 36 Zentralanstalt für Meteorologie und Geodynamik, 1190 Wien, Austria.  
 37 m. National Center for Atmospheric Research, Boulder, CO, US.  
 38 n. Center of Excellence SPACE-SI, Ljubljana, Slovenia.  
 39 o. Air Quality Research Section, Atmospheric Science and Technology Directorate,  
 40 Environment Canada, 4905 Dufferin Street, Toronto, Ontario, Canada.  
 41 p. Met Office, FitzRoy Road, Exeter, EX1 3PB, United Kingdom.  
 42 q. Environmental Software and Modelling Group, Computer Science School - Technical  
 43 University of Madrid, Campus de Montegancedo - Boadilla del Monte-28660, Madrid,  
 44 Spain.

- 45 r. Emissions and Model Evaluation Branch, Atmospheric Modeling and Analysis  
46 Division/NERL/ORD, Research Triangle Park, North Carolina, USA.  
47 s. Leibniz Institute for Tropospheric Research, Permoserstr. 15, D-04318 Leipzig,  
48 Germany.  
49 t. National Institute of Meteorology and Hydrology, Bulgarian Academy of Sciences, 66  
50 Tzarigradsko shaussee Blvd., Sofia 1784, Bulgaria.  
51 u. Department of Marine, Earth and Atmospheric Sciences, North Carolina State  
52 University, Raleigh, USA.  
53 v. University of Ljubljana, Faculty of Mathematics and Physics, Ljubljana, Slovenia.

54  
55 \* Corresponding author: S. Galmarini ([Stefano.galmarini@jrc.ec.europa.eu](mailto:Stefano.galmarini@jrc.ec.europa.eu))  
56

## 57 Highlights

- 58
- 59 • Seventeen modeling groups from EU and NA simulated PM for 2010 under AQMEII  
60 phase 2
- 61 • A general model underestimation of surface PM over both continents up to 80%
- 62 • Natural PM emissions may lead to large underestimations in simulated PM<sub>10</sub>.
- 63 • Dry deposition can introduce large differences among models.
- 64
- 65

66 Keywords: AQMEII, on-line coupled models, performance analysis, particulate matter,  
67 Europe, North America

## 68 ABSTRACT

69  
70  
71 The second phase of the Air Quality Model Evaluation International Initiative (AQMEII)  
72 brought together seventeen modeling groups from Europe and North America, running eight  
73 operational online-coupled air quality models over Europe and North America using common  
74 emissions and boundary conditions. The simulated annual, seasonal, continental and sub-  
75 regional particulate matter (PM) surface concentrations for the year 2010 have been evaluated  
76 against a large observational database from different measurement networks operating in  
77 Europe and North America. The results show a systematic underestimation for all models in  
78 almost all seasons and sub-regions, with the largest underestimations for the Mediterranean  
79 region. The rural PM<sub>10</sub> concentrations over Europe are underestimated by all models by up to  
80 66% while the underestimations are much larger for the urban PM<sub>10</sub> concentrations (up to  
81 75%). On the other hand, there are overestimations in PM<sub>2.5</sub> levels suggesting that the large  
82 underestimations in the PM<sub>10</sub> levels can be attributed to the natural dust emissions. Over  
83 North America, there is a general underestimation in PM<sub>10</sub> in all seasons and sub-regions by  
84 up to ~90% due mainly to the underpredictions in soil dust. SO<sub>4</sub><sup>2-</sup> levels over EU are  
85 underestimated by majority of the models while NO<sub>3</sub><sup>-</sup> levels are largely overestimated,  
86 particularly in east and south Europe. NH<sub>4</sub><sup>+</sup> levels are also underestimated largely in south  
87 Europe. SO<sub>4</sub> levels over North America are particularly overestimated over the western US  
88 that is characterized by large anthropogenic emissions while the eastern USA is characterized  
89 by underestimated SO<sub>4</sub> levels by the majority of the models. Daytime AOD levels at 555nm is  
90 simulated within the 50% error range over both continents with differences attributed to  
91 differences in concentrations of the relevant species as well as in approaches in estimating the

92 AOD. Results show that the simulated dry deposition can lead to substantial differences  
93 among the models. Overall, the results show that representation of dust and sea-salt emissions  
94 can largely impact the simulated PM concentrations and that there are still major challenges  
95 and uncertainties in simulating the PM levels.

96  
97

## 98 1. Introduction

99 Particulate matter (PM) is related to respiratory and cardiovascular diseases as well as to  
100 mortality (Schwartz et al., 1996; Bernard et al., 2001). PM has direct and indirect effects on  
101 climate (IPCC, 2007) and in turn, climate may have a significant impact on PM levels and  
102 composition (Jacob and Winner, 2009). PM has both anthropogenic and natural sources and  
103 are emitted as primary aerosols or are chemically formed from gaseous precursors in the  
104 atmosphere. PM levels are still a concern, particularly in the urban areas and its adverse  
105 effects on climate and health are expected to persist (Klimont et al., 2009; Winker et al.,  
106 2013). Due to the greater potential of PM<sub>2.5</sub> (PM with an aerodynamic diameter smaller than  
107 2.5  $\mu\text{m}$ ) to cause adverse effects on public health compared to PM<sub>10</sub> (PM with an aerodynamic  
108 diameter below 10  $\mu\text{m}$ ), PM<sub>2.5</sub> attracted more scientific attention that led to air quality model  
109 (AQM) development to focus more on this size of PM and its composition. PM can lead to  
110 reductions in radiation reaching the earth and therefore impact the temperature, wind speed  
111 and humidity, and it can also modify cloud droplet size and number (Baklanov et al., 2014;  
112 Brunner et al., 2014). On-line coupled AQMs can simulate the aerosol feedbacks on  
113 meteorology that can be important on a wide range of temporal and spatial scales (Zhang  
114 2008; Grell and Baklanov, 2011).

115 The Air Quality Model Evaluation International Initiative (AQMEII) is designed to promote  
116 policy-relevant research on regional air quality model evaluation across the atmospheric  
117 modeling communities in Europe (EU) and North America (NA) through the exchange of  
118 information on current practices and the identification of research priorities (Galmarini and  
119 Rao, 2011). Standardized observations and model outputs were made available through the  
120 ENSEMBLE web-based system (<http://ensemble2.jrc.ec.europa.eu/public/>) that is hosted at  
121 the Joint Research Centre (JRC; Bianconi et al., 2004; Galmarini et al., 2012). The first phase  
122 of AQMEII focused on the evaluation of off-line atmospheric modelling systems against large  
123 sets of monitoring observations over Europe and North America for the year 2006 (Solazzo et  
124 al., 2012a,b and 2013; Vautard et al., 2012; Hogrefe et al., 2014). The results from this first  
125 phase demonstrated a large underestimation by all models throughout the year and a large  
126 variability among models in representing emissions, deposition and concentrations of PM and  
127 their composition (Solazzo et al., 2012b).

128 The second phase of AQMEII extends this model assessment to on-line air quality models. In  
129 this study, we analyze PM<sub>10</sub> and PM<sub>2.5</sub> mass concentrations simulated by eight on-line-  
130 coupled models, which have been run by seventeen independent groups from Europe and  
131 North America (a companion study is devoted to the analyses of ozone, Im et al., 2014). The  
132 surface PM levels simulated by the individual models as well as their ensemble mean and

133 median are compared with the observational data provided by the ENSEMBLE system. As  
134 multi-model ensemble analyses is not the scope of this paper, further analyses have been  
135 performed by Kioutsioukis et al. (2014) for the EU case using the multi-model data presented  
136 in the present paper. The aim of the study is to evaluate the performances of widely used  
137 operational on-line coupled models in EU and NA in simulating PM and its chemical  
138 components on a sub-regional and seasonal basis employing an experimental set up with  
139 common anthropogenic emission and boundary conditions and thus, to identify areas of model  
140 improvements and the links to policy applications.

141

## 142 2. Materials and Methods

### 143 2.1. Models

144 In the context of AQMEII2, thirteen modeling groups from EU and four modeling groups  
145 from NA have submitted PM simulations for the year 2010 (Table 1). One European group  
146 (BG2) employed an off-line coupled model while the rest of the groups performed their  
147 simulations using their operational on-line models. Nine groups used WRF/CHEM model  
148 (Grell et al., 2005) and its variant (e.g. Wang et al., 2014), having different gas-phase  
149 mechanisms (see Table 1 in Im et al., 2014) but similar aerosol modules that employ different  
150 size distributions approaches (modal/bin) and inorganic/organic aerosol treatments as seen in  
151 Table 1. The IT2 simulation is performed with an experimental version of WRF/Chem v. 3.4,  
152 where the new secondary organic aerosol scheme VBS was coupled to the aerosol indirect  
153 effects modules. Therefore, the bias of IT2 run should not be regarded as the bias of the  
154 general WRF/Chem modeling system, but only of this particular version under development.  
155 The simulations were conducted for continental-scale domains of EU and NA covering  
156 continental U.S., southern Canada and northern Mexico (Fig.1). To facilitate the cross-  
157 comparison between models, the participating groups interpolated their model output to a  
158 common grid with  $0.25^\circ$  resolution for both continents. Model values at observation locations  
159 were extracted from the original model output files for comparison to observations (described  
160 below).

### 161 2.2. Emissions and Boundary Conditions

162 Standard anthropogenic emissions were provided by the TNO (Netherlands Organization for  
163 Applied Scientific Research) for EU (Kuenen et al., 2014) and by U.S. EPA (United States  
164 Environmental Protection Agency) and Environment Canada for NA (Pouliot et al., 2014).  
165 The NA emissions were processed by the US EPA for all models except for GEM-MACH,  
166 where a different grid projection required separate processing by Environment Canada.  
167 Different assumptions were used for snow reduction of fugitive dust emissions in these two  
168 efforts. More information on the implementation of these emissions is provided in Im et al.  
169 (2014). The spatial distribution of annually-integrated anthropogenic  $PM_{2.5}$  emissions for EU  
170 and NA domains are depicted in Fig.1. Anthropogenic  $PM_{10}$  emissions per  $km^2$  in NA ( $76$   
171  $ktons\ km^{-2}\ yr^{-1}$ ) are larger than those in EU ( $69\ ktons\ km^{-2}\ yr^{-1}$ ) while EU is characterized by  
172 larger  $PM_{2.5}$  emissions density ( $49\ ktons\ km^{-2}\ yr^{-1}$ ) compared to NA ( $29\ ktons\ km^{-2}\ yr^{-1}$ ). EU



173 also has more than a factor of two larger NO<sub>x</sub>, NMVOC and NH<sub>3</sub> emission densities  
174 compared to NA (Im et al., 2014). Note that the emissions over the oceans represent those  
175 originating only from the maritime sector (Kuenen et al., 2014; Pouliot et al., 2014). Fig.1  
176 also shows the monthly variation of PM<sub>2.5</sub> emissions over EU and NA. There is a clear  
177 seasonal variation in EU emissions. Spring season is characterized with the highest emissions  
178 in both domains. The PM speciation profiles for EU are based on Kulmala et al. (2011) while  
179 the temporal profiles for the EU anthropogenic emissions are based on Schaap et al. (2005).  
180 Each modeling group used their own biogenic (see Table 1 in Im et al., 2014), dust, and sea-  
181 salt emission modules in their operational model as seen in Table 1. Hourly biomass burning  
182 emissions were provided by Finnish Meteorological Institute (FMI) fire assimilation system  
183 (<http://is4fires.fmi.fi/>; Sofiev et al., 2009; Soares et al., 2014). 3-D daily chemical boundary  
184 conditions were provided by the ECMWF IFS-MOZART model (referred as MACC  
185 hereafter) run in the context of the MACC-II project (Monitoring Atmospheric Composition  
186 and Climate – Interim Implementation) on 3-hourly and 1.125° spatial resolution (Inness et  
187 al., 2013). The aerosol chemical species available in the reanalysis included sea-salt, dust,  
188 organic matter, black carbon and sulfate. However, following the AQMEII Phase 1 experience  
189 described in Schere et al. (2012), MACC-II sea-salt concentrations were not used as chemical  
190 boundary conditions for the NA domain.

### 191 2.3. Observations

192 Observations of hourly and daily rural and urban surface PM<sub>10</sub> and PM<sub>2.5</sub> mass concentrations  
193 with a data availability of at least 75% from different measurement networks in EU (EMEP  
194 (European Monitoring and Evaluation Programme; <http://www.emep.int/>) and AirBase  
195 (European AQ database; <http://acm.eionet.europa.eu/databases/airbase/>)) and NA (the  
196 Canadian National Atmospheric Chemistry (NAtChem) Database and Analysis Facility  
197 operated by Environment Canada (<http://www.ec.gc.ca/natchem/>) that contains measurements  
198 from the Canadian National Air Pollution Surveillance Network ([http://maps-  
200 cartes.ec.gc.ca/rmspa-naps/data.aspx](http://maps-<br/>199 cartes.ec.gc.ca/rmspa-naps/data.aspx)), the Canadian Air and Precipitation Monitoring Network  
201 (<http://www.ec.gc.ca/natchem/>), the U.S. Clean Air Status and Trends Network  
202 (<http://java.epa.gov/castnet/clearsession.do>), the U.S. Interagency Monitoring of Protected  
203 Visual Environments Network (<http://views.cira.colostate.edu/web/DataWizard/>), and the  
204 U.S. Environmental Protection Agency's Air Quality System database for U.S. air quality data  
205 (<http://www.epa.gov/ttn/airs/airsaqs/detaildata/downloadaqsddata.htm>)) have been used in  
206 order to evaluate the model performances in simulating the surface PM concentrations in the  
207 two continents (Figure 1). Daily averages were calculated using the hourly observations from  
208 the station where daily measurements were not available and the analyses were performed on  
209 the daily averaged PM concentrations. Daily observations from 1525 stations (439 rural and  
210 1076 urban) in EU and 469 stations (158 rural and 311 urban) in NA were used for PM<sub>10</sub>  
211 comparisons. For PM<sub>2.5</sub>, data from 517 stations in EU (139 rural and 378 urban) and 659  
212 stations in NA (311 rural and 348 urban) were used. A geographical breakdown into three  
213 sub-regions for each continent that is similar to that in Solazzo et al. (2012) was applied,  
214 which is based on emission and climatological characteristics (Fig.1). The European sub-  
215 region EU1 can be characterized by north-western European sources with a transition climate  
between marine and continental and hosts 618 stations for PM<sub>10</sub> (216rural and 402 urban) and

216 255 stations for  $PM_{2.5}$  (66 rural and 189 urban). EU2 covers the north-eastern and central  
217 Europe sources as well as Germany with 433 stations for  $PM_{10}$  (124 rural and 309 urban) and  
218 124 stations for  $PM_{2.5}$  (21 rural and 103 urban). EU3 is characterized by the Mediterranean  
219 type climate and sources covering 375 stations for  $PM_{10}$  (92 rural and 283 urban) and 94  
220 stations for  $PM_{2.5}$  (44 rural and 50 urban). Sub-region NA1 consists of the arid southwestern  
221 part of the U.S. with the western slope of the Rocky mountains on the east and hosts 113  
222 stations for  $PM_{10}$  (44 rural and 69 urban) and 70 stations for  $PM_{2.5}$  (37 rural and 33 urban).  
223 NA2 covers the more humid south eastern U.S. with 45 stations for  $PM_{10}$  (17 rural and 28  
224 urban) and 117 stations for  $PM_{2.5}$  (52 rural and 65 urban). NA3 consists of the northeastern  
225 NA that is characterized by the highest emission sources in NA covering 64 stations for  $PM_{10}$   
226 (11 rural and 53 urban) and 188 stations for  $PM_{2.5}$  (78 rural and 110 urban).

## 227 2.4. Statistical analyses

228 A number of statistical parameters, including Pearson's correlation coefficient ( $PCC$ ), root  
229 mean square error ( $RMSE$ ); normalized mean standard error ( $NMSE$ ) and normalized mean  
230 bias ( $NMB$ ) are calculated (Im et al., 2014) in order to compare the individual model  
231 performances as well as the ensemble mean and median. The comparisons are performed  
232 individually for the two domains and their sub-regions for the whole simulation period and on  
233 a seasonal basis, in order to identify which regions and/or seasons have systematic errors.

234

## 235 3. Results and Discussion

### 236 3.1. $PM_{10}$

#### 237 3.1.1. Seasonal and regional surface levels over Europe

238 Comparisons of observed and simulated annual and domain-averaged  $PM_{10}$  and  $PM_{2.5}$   
239 concentrations over the rural and urban monitoring stations in EU and NA are presented in  
240 Table 2. The temporal variation of the rural  $PM_{10}$  levels over EU are moderate-to-well-  
241 reproduced by the models ( $PCC=0.18-0.86$ ), while the variations at urban sites were  
242 reproduced with slightly lower agreement ( $PCC=0.06-0.82$ ). For both station types, the  
243 lowest correlations are calculated for DE4, ES1 and UK4 ( $PCC<0.25$ ) while BG2 and UK5  
244 well-captured the variation of  $PM_{10}$  with  $PCC$  larger than 0.75. The monthly time series plots  
245 presented in Fig.2 and 3 (upper panels) also show that particularly in winter, the monthly  
246 temporal variations were not captured by any of the models while they mainly follow the  
247 temporal evolution introduced by the MACC model that provides the chemical boundaries.  
248 The figures show that the majority of the models produced spring and autumn peaks,  
249 particularly for the rural stations while these are not observed in the measurements or the  
250 MACC model, suggesting that the anthropogenic PM emissions or the online-simulated  
251 natural dust emissions can be responsible for these peaks. Over EU, the rural  $PM_{10}$   
252 concentrations are underestimated by all models from 10% (UK4) to 66% (IT2). The  
253 underestimations are much larger for the urban  $PM_{10}$  concentrations ranging from 43% (UK4)  
254 to 75% (IT2), suggesting that the urban emissions were not able to represent the actual



emissions, given the coarse resolution of the models. The underestimations are in all percentiles as can be seen in the box-and-whisker plots presented in Fig.4. The figure also shows that the variability in the models are much lower compared to the observed variability except for UK4 for the rural levels, which has the lowest bias for both station types. The general tendency of all models to underestimate observed  $PM_{10}$  concentrations may be at least partially attributable to sub-grid scale effects since monitors may be located near hot spots and may introduce substantial horizontal gradients near such hot spot locations.

Regarding sub-regional rural  $PM_{10}$  levels, the highest biases are calculated for EU2 ( $NMB=-34\%$  to  $-75\%$ ), which is characterized by large anthropogenic emissions while EU1 and EU3 have relatively smaller biases ( $-10\%$  to  $-63\%$  and  $-12\%$  to  $-57\%$ , respectively). The temporal variability is best captured for the sub-region EU1 with  $PCC$  values between 0.4 and 0.9 and lowest in the sub-region EU2 ( $PCC=0.2$  to 0.9). Similar to the continental scale (EU0), in all sub-regions, the smallest biases are calculated for the UK4 model while the largest are calculated for the IT2 model. For the urban  $PM_{10}$  levels, EU2 and EU3 have the largest biases (up to  $-81\%$ ). UK4 model has the lowest  $MNB$  values while IT2 model is again associated with the largest biases. The temporal variation was best reproduced by the UK5 model for all sub-regions except for EU3 where highest  $PCC$  is calculated for IT1 model.

The seasonal and regional model evaluations are conducted through soccer plots presented in Figs.5 and 6, summarizing the performance in both domains for the rural and urban sites, respectively. The observed and modeled surface rural  $PM_{10}$  levels over EU are compared in Fig.5a-d (upper panel). The results show a systematic underestimation for all models in almost all seasons and sub-regions. The largest underestimations for the rural  $PM_{10}$  are calculated for the EU3 sub-region (Mediterranean), particularly during winter (Fig.5a). In sub-region EU1, underestimations of 2% (in summer by SII) to 74% (in winter by IT2) are calculated. In EU1, surface  $PM_{10}$  levels in autumn were overestimated by 1% and 4% by IT1 and SII, respectively. In sub-region EU2, the highest underestimation (85%) was calculated for IT2 model again for the winter period (Fig.5a) while SII model had the smallest underestimations with values from 23% to 57%. UK4 model had the lowest underestimations for the spring and summer levels (Fig.5a,d) by 14% and 11%, respectively. Overall, the largest biases were calculated for the winter period (by up to 85%). Similar results were calculated for the urban surface  $PM_{10}$  levels in EU with slight lower biases (Fig.6a-d).

### 3.1.2. Seasonal vs regional surface levels over North America

Over NA, the temporal variation of rural  $PM_{10}$  levels is poorly reproduced by majority of the models with  $PCC$  of 0.22 to 0.38 (Table 2). CA2f model fails to reproduce the temporal variation ( $PCC=-0.05$ ). The low values for this last model may be due to the lack of snow reduction factors in the reprocessing of emissions of fugitive dust for this model in this experiment (see Pouliot et al, 2014). On the other hand, the temporal variation at the urban sites are slightly better captured by the models ( $PCC=0.18-0.54$ ). The  $NMB$  values do not differ much between the rural and urban stations on the continental scale (NA0) as seen in Table 2. Over both station types, ES1 and US8 models have the largest biases ( $>70\%$ ) while other models have much lower biases ( $<40\%$ ). The monthly variations in NA0 (NA0) are

296 better captured compared to the daily variability as seen in Figs.2 and 3. In sub-region NA1,  
297 particularly over the rural stations, the majority of the models fail to reproduce both the  
298 temporal variation and the magnitudes. In sub-regions NA2 and NA3, the temporal variability  
299 is relatively better captured by the models. The variability in the observed  $PM_{10}$   
300 concentrations are relatively well represented by CA2f and US7 with low biases ( $< 20\%$ ) as  
301 seen in Fig.4 (upper panel), but also by US6 with a larger bias over the rural ( $-39\%$ ) and urban  
302 ( $-34\%$ ) stations (Table 2). Similar to the EU domain, the MACC model largely underpredicts  
303 the observed variability.

304 The temporal variability of rural  $PM_{10}$  levels over the NA1 sub-region was poorly reproduced  
305 by all models with  $PCC$  values ranging from 0.03 (CA2f) to 0.52 (US6). In NA2,  $PCC$  values  
306 were also low;  $-0.16$  (ES1) to  $0.56$  (US7). Temporal variations over NA3, however, were  
307 reproduced reasonably well by most models ( $PCC=0.69$  to  $0.74$ ) except for the ES1 model  
308 ( $PCC=0.28$ ). There is a general underestimation by all models in all sub-regions. As can be  
309 seen in Fig.2, the largest underestimation occurs in NA1 ( $MNB=-57\%$  to  $-84\%$ ) with the  
310 exception of US7 overestimating by  $19\%$ . Over NA2 and NA3, underestimations from  $20\%$  to  
311  $88\%$  are calculated. The largest underestimations are calculated for ES1 ( $MNB>80\%$ ) while  
312 US7 had the smallest biases ( $<25\%$ ). Urban  $PM_{10}$  levels over NA are best reproduced in NA3  
313 with  $PCC$  over  $0.60$  except for ES1 ( $PCC=0.33$ ).  $PCC$  values range from  $0.11$  to  $0.55$  over  
314 NA1 and from  $-0.15$  to  $0.72$  over NA2. There are generally underestimations by up to  $87\%$  in  
315 the sub-regions while CA2f and US7 overestimate the urban  $PM_{10}$  levels over NA1 by  $11\%$   
316 and  $20\%$ , respectively. The largest biases are calculated for the ES1 model in all sub-regions  
317 ( $MNB=80\%$  to  $87\%$ ).

318 Soccer plots for the seasonal and geographical model performance for the rural and urban  
319 surface  $PM_{10}$  levels over NA are presented in Figs.5 and 6 (lower panels). Over NA, there are  
320 no systematic seasonal trends in model performance except for the ES1 and US8 models  
321 having the largest biases for rural  $PM_{10}$  levels in all seasons and sub-regions (Fig.5e-h). ES1  
322 model follows US8 with slightly lower biases. The largest underestimations were calculated  
323 for the spring and summer periods in all sub-regions by up to  $90\%$  and  $93\%$ , respectively.  
324 There is a general underestimation in all seasons and sub-regions, with the exception of  
325 overestimations calculated for US7 model by  $3\%$  to  $67\%$  over NA1. On a continental scale,  
326 US7 model slightly overestimates the rural  $PM_{10}$  levels by  $3\%$ . The model performances for  
327 the urban  $PM_{10}$  levels over NA (Fig.6e-h) are similar to those for the rural levels, with slightly  
328 lower biases.

329 The large differences in  $PM_{10}$  predictions among those models and their performances at rural  
330 and urban sites can be attributed mainly to the use of different online dust emission modules.  
331 For example, US7 and US8 use two different dust emission modules available in WRF/Chem  
332 version 3.4.1, i.e., the MOSAIC/GOCART dust module of Zhao et al. (2010) and  
333 AER/AFWA dust module of Jones and Creighton (2011). The simulated coarse dust  
334 concentrations by the two dust emission modules used by US7 and US8 are significantly  
335 different in terms of locations and magnitudes (Fig.S1). While both simulate dust emissions  
336 from the Mojave desert in southeastern California and the Sonoran Deserts in southern  
337 Arizona, the MOSAIC/GOCART dust module gives much higher coarse dust emissions than

338 the AER/AFWA dust module in these areas with a much broader areal coverage and also  
339 predict dust emissions in many other areas in the continental U.S. and northern Mexico. As  
340 reported by Raman and Arellano (2013), the AER/AFWA dust emission module in  
341 WRF/Chem v. 3.4.1 significantly underpredicted dust emissions over Phoenix area in  
342 Arizona, U.S., resulting in significant underpredictions of  $PM_{10}$  ( $\sim 50 \text{ mg m}^{-3}$ ) comparing to  
343 the observed concentration of  $1800 \mu\text{g m}^{-3}$ . While differences in the dust emission modules  
344 explain most differences in coarse dust, another reason for much lower dust concentrations by  
345 US8 is the use of a simplified surface drag parameterization of Mass and Ovens (2010).  
346 While this parameterization helps reduce the overpredictions of wind speeds (Wang et al.,  
347 2014; Yahya et al., 2014a, b), it reduces dust emissions which depend strongly on wind  
348 speeds. The sensitivity simulation without the parameterization of Mass and Ovens (2010)  
349 gives dust concentrations that are higher by about a factor of two than the one with this  
350 parameterization. The substantial differences in coarse dust concentrations contribute to large  
351 differences in coarse PM between the two model simulations. Differences in sea-salt  
352 emissions predicted by US7 and US8 also contribute to differences in coarse PM  
353 concentrations, although their contributions to differences in  $PM_{10}$  performance at rural and  
354 urban locations are negligible (in particular, for sites located inland). Although US7 and US8  
355 use the same sea-salt emission module of Gong et al. (1997), US8 gives lower sea-salt  
356 emissions (thus lower sea-salt concentrations) over oceanic areas because of the use of a  
357 simplified surface drag parameterization of Mass and Ovens (2010) that gives lower wind  
358 speeds.

## 359 3.2. $PM_{2.5}$

### 360 3.2.1. Seasonal and regional surface levels over Europe

361 All models show a very similar behavior for simulated continental surface rural and urban  
362  $PM_{2.5}$  levels compared to the simulated  $PM_{10}$  levels, with lower biases, as seen in the box-  
363 and-whisker plots presented in the lower panel of Fig.4. *PCC* values calculated for the  
364 simulated  $PM_{2.5}$  levels are very similar in general to those calculated for the  $PM_{10}$  levels  
365 (Table 2). Over the rural stations, the underestimations range from 2% (CH1) to 60%, with the  
366 highest bias calculated for the IT2 model similar to  $PM_{10}$ . For the urban stations, the largest  
367 bias was again calculated for the IT2 model ( $MNB=68\%$ ). UK4 model overestimated the rural  
368  $PM_{10}$  concentrations by 20% (Table 2) as can also be seen in Fig.7. The sub-regional analyses  
369 show that these overestimations are mostly due to the large overestimations particularly  
370 during summer in the Mediterranean region (EU3) by up to 72%. Further analyses have  
371 shown that these overestimates for UK4 are due to excessive model PM from wildfire  
372 emissions on the Iberian Peninsular where the vast majority of PM observations are located.  
373 The UK4 model has not previously been run for a domain with large sources of wildfires and  
374 it seems likely that the implementation of these sources needs further improvement in this  
375 model configuration. The MACC model underestimates the continental and annual mean  
376 levels as shown in Fig.4, as well as in all sub-regions and seasons, suggesting that these  
377 overestimations are not due to the boundary conditions, but may be due to the emissions or  
378 deposition. Dry deposition of  $PM_{2.5}$  calculated by the models (Fig.9a) show that IT2 and SII  
379 models simulate significantly larger deposition compared to the other models. This can

380 explain the systematic largest underestimations associated with the IT2 model compared to  
381 the other models.

382 The soccer plots presented in Fig.10a and 11a show that winter levels are underestimated by  
383 all models in all sub-regions, in general by more than 50%, particularly over the urban  
384 stations. In other seasons, the underestimations are lower. CH1 and UK4 models overestimate  
385 in spring and in particular during summer. IT1 and SI1 overestimate rural EU3 PM<sub>2.5</sub> levels  
386 by 4% and 5%, respectively (Fig.10b). Similar overestimations hold for UK4 over the urban  
387 stations (Fig.11b). In summer, there is general underestimation by the majority of the models  
388 by up to 49% and 59% (by IT2 in EU2) over the rural and urban stations, respectively  
389 (Fig.10c and 11c). Autumn levels are underestimated by up to 72% over the rural (Fig.10d)  
390 and by up to 77% over the urban stations (Fig.11d) depending on the region with the  
391 maximum bias calculated for EU2 by the IT2 model.

### 392 3.2.2. Seasonal vs regional surface levels over North America

393 The temporal variations for the domain-averaged surface PM<sub>2.5</sub> concentrations over both rural  
394 and urban stations are much better captured by the majority of the models compared to the  
395 PM<sub>10</sub> levels (Table 2). *PCC* values for the urban stations (0.31 to 0.78) are higher than those  
396 for the rural values (0.05 to 0.61) for all models, as can also be seen from the monthly time  
397 series plots in Fig.7 and 8. ES1 model had the lowest correlations while US7 had the highest  
398 values. ES1 model also had the largest biases (*MNB*=-68% and -71% for rural and urban  
399 stations, respectively) while US8 simulated the surface PM<sub>2.5</sub> levels with the lowest bias  
400 (*MNB*=-26% and -17%, respectively). The large underestimation calculated for the ES1 model  
401 can be attributed to the significantly larger dry deposition compare to the other models as can  
402 be seen in Fig.9b. As discussed in section 3.1.2, the underestimation in the PM<sub>10</sub> levels for the  
403 US8 model suggests that the dust particles in both coarse and fine modes are significantly  
404 underestimated by this model. US7 model overestimated the domain-averaged PM<sub>2.5</sub> levels  
405 over both station types by ~48%, likely due to an overprediction in dust and sea-salt  
406 concentrations in PM<sub>2.5</sub> size sections. PM<sub>2.5</sub> concentrations predicted by US7 are much higher  
407 than those from US8 (Fig.S1). Such differences can be attributed to several factors. First,  
408 US7 and US8 use different dust emission modules, which give very different concentrations  
409 of dust in the PM<sub>2.5</sub> size sections/modes. Second, US7 and US8 use different splitting  
410 fractions between coarse and fine dust emissions. US7 allocates 9% and 68% of the total dust  
411 emission to PM<sub>2.5</sub> and coarse PM, respectively. Since MOSAIC only describes aerosols up to  
412 10 µm, the emissions for particles with diameter greater than 10 µm are neglected (which is  
413 23% of the total emissions). For comparison, US8 allocates 3% of dust emissions in the  
414 accumulation mode and the rest of 97% in the coarse mode. Third, US7 and US8 give  
415 different predictions of primary and secondary organic aerosols (POA and SOA), due possibly  
416 to the use of different SOA modules and different conversion factors between primary organic  
417 carbon emissions and the POA simulated in the model. As seen in Fig.4, the models have  
418 similar profiles for both rural and urban stations while the MACC model overestimates the  
419 rural and underestimates the urban PM<sub>2.5</sub> concentrations, implying that the simulated levels  
420 were due to local contributions rather than regional transport.



421 US7 model overestimates both the rural and urban PM<sub>2.5</sub> concentrations in all seasons and  
 422 sub-regions (Fig.10 and 11e-h). The overestimations simulated by US7 model are smallest  
 423 during winter from 16% to 96% over the rural and 51% to 82% over the urban stations. The  
 424 figures also show that ES1 model underestimates in all seasons and sub-regions. With the  
 425 exception of ES1 model, all models fall into the 75% error range in all seasons and sub-  
 426 regions, while excluding US7, the error decreases to the 50% range (Fig.10 and 11e-h).  
 427 Compared to the PM<sub>10</sub> levels, the figures show that majority of the models are grouped around  
 428 the zero line of the soccer plots. The differences in all seasons are highest in sub-region  
 429 NA1 over both rural (*MNB* up to 143%) and urban stations (*MNB* up to 95%).

### 430 3.2.3. PM<sub>2.5</sub> speciated components

431 Simulated surface sulfate (SO<sub>4</sub><sup>2-</sup>), nitrate (NO<sub>3</sub><sup>-</sup>) and ammonium (NH<sub>4</sub><sup>+</sup>) components of PM<sub>2.5</sub>  
 432 aerosols are compared with observations from five, six, and five rural stations in EU,  
 433 respectively, and 250, 148 and 149 station in NA, respectively. The results are presented in  
 434 Fig.12 in the soccer plots for the continental and sub-regional levels in 2010 over EU and NA.  
 435 Over EU, the continental SO<sub>4</sub><sup>2-</sup> levels are underestimated by a majority of the models (AT1,  
 436 DE4, ES1, ES3, IT1, IT2 and UK5) by 22% to 61% (Fig.12a) while few groups (BG2, CH1,  
 437 NL2, SII and UK4) overestimated the SO<sub>4</sub><sup>2-</sup> levels by 7% to 52%. The results show that the  
 438 underestimating models were all WRF/CHEM models, with the exception of SII that  
 439 overestimates. The largest underestimation of SO<sub>4</sub><sup>2-</sup> by IT2 can be attributed to the large SO<sub>4</sub><sup>2-</sup>  
 440 dry deposition calculated by this model (Fig.9a). SO<sub>4</sub><sup>2-</sup> underestimation can also be attributed  
 441 to absence of SO<sub>2</sub> oxidation in cloud water in the heterogeneous phase (e.g. the IT1 model:  
 442 Balzarini et al., 2014). As seen in Fig.12b and c, simulated NO<sub>3</sub><sup>-</sup> and NH<sub>4</sub><sup>+</sup> are higher than the  
 443 observed levels. NO<sub>3</sub><sup>-</sup> levels are overestimated by majority of the models in all regions by  
 444 more than 75%, particularly in EU2 and EU3 (Fig.12b). NH<sub>4</sub><sup>+</sup> levels are also underestimated  
 445 largely in EU3. In other sub-regions, the differences for simulated NH<sub>4</sub><sup>+</sup> levels are lower (50%  
 446 to 75%). The results suggest ammonium nitrate (NH<sub>4</sub>NO<sub>3</sub>) formation dominating over the  
 447 ammonium sulfate ((NH<sub>4</sub>)<sub>2</sub>SO<sub>4</sub>) formation over EU as well as possible underestimations in  
 448 heterogeneous (cloud) SO<sub>4</sub> formation and generation of fine sea-salt emissions.

449 The picture is completely opposite over the NA domain as seen in Fig.12d-f. SO<sub>4</sub><sup>2-</sup> levels are  
 450 particularly overestimated over NA1 as well as over the continent. Particularly CA2f model  
 451 largely overestimates SO<sub>4</sub><sup>2-</sup> levels in all sub-regions. NA2 and NA3 are characterized by  
 452 underestimated SO<sub>4</sub><sup>2-</sup> levels by the majority of the models. The differences from the  
 453 observations are in general below 75% except for the CA2f model that has much larger bias.  
 454 CA2f model has the smallest differences for both NO<sub>3</sub><sup>-</sup> and NH<sub>4</sub><sup>+</sup> while ES1 model has the  
 455 largest underestimations by more than a factor of 2.

### 456 3.3. Aerosol Optical Depth (AOD)

457 The reconstructed AOD at 555nm (AOD555) are compared with observations from 35  
 458 Aerosol Robotic Network (AERONET; [http://aeronet.gsfc.nasa.gov/new\\_web/index.html](http://aeronet.gsfc.nasa.gov/new_web/index.html))  
 459 stations from each domain. Soccer plots and the diurnal profiles for the model performances  
 460 in 2010 for the continental and sub-regional AOD555 levels are presented in Fig.13a,c. Over  
 461 EU (Fig.12a), the majority of the model performed within the 50% error range. The DE3

462 model had the largest underestimations ( $MNB=60\%$ ) in all regions (Fig.13c) while the BG2  
463 model had the largest overestimations ( $MNB$  up to  $70\%$ ). The large underestimation by the  
464 DE3 model can be attributed to the approach in estimating the AOD555. While the majority  
465 of the models consider  $SO_4$ ,  $NO_3$ ,  $NH_4$ , primary and secondary organic aerosols  
466 (POA/SOA), elemental carbon (EC), dust and sea-salt (Curci et al., 2014) in their AOD  
467 estimations, the DE3 model does not consider EC, POA/SOA and sea-salt. The smallest bias  
468 was calculated for SI1 ( $MNB=+7\%$ ) and for AT1 ( $-12\%$ ). In general, models BG2, CH1, NL2  
469 and UK5 overestimated the observed AOD555 levels while other models underestimate. The  
470 observed hourly diurnal variation over the continent was moderately captured by the models  
471 with a maximum and minimum  $PCC$  of 0.65 (AT1) and 0.25 (DE3), respectively.  
472 WRF/CHEM models were associated with very similar temporal variations ( $PCC\sim 0.6$ ). Over  
473 NA (Fig.13b,d), CA2f model failed to reproduce both the temporal variation ( $PCC=0.23$ ) and  
474 the magnitude of the continental AOD555 with an overestimation of 29%. US6 model  
475 reproduced the temporal variation better than the other models ( $PCC=0.73$ ), but with the  
476 largest bias ( $MNB=-32\%$ ). US7 also overestimated the continental AOD555 by 25% and  
477 captured the temporal variability ( $PCC=0.70$ ) while US8 underestimated the observations by  
478 17% with a temporal agreement of 0.65. Further discussion on model uncertainty on AOD  
479 calculation may be found in Curci et al. (2014).

480

#### 481 4. Summary and Conclusions

482 An operational evaluation of simulated particulate matter (PM) levels over Europe (EU) and  
483 North America (NA) in 2010 using eight different on-line-coupled air quality models from  
484 sixteen groups has been conducted in the context of the AQMEII project. Seven groups from  
485 EU and two groups from NA applied the WRF/CHEM model, but with different settings.  
486 Anthropogenic emissions and chemical boundary conditions were prescribed while biogenic  
487 emissions were calculated online by each individual group. All groups interpolated their  
488 model output to a common output grid and a common set of receptor locations and uploaded  
489 the data to the ENSEMBLE system. The results are evaluated against surface and sounding  
490 observations, which are provided by operational over EU and NA, at continental and sub-  
491 regional levels on annual and seasonal basis.

492 Results show that over EU, particularly in winter, the monthly temporal variations were not  
493 captured by any of the models while the majority of the models produced spring and autumn  
494 peaks, particularly for the rural stations while these are not observed in the measurements or  
495 the MACC model, suggesting that the anthropogenic emissions or the online-simulated  
496 natural dust emissions can be responsible for these peaks. Over EU, the rural  $PM_{10}$   
497 concentrations are underestimated by all models by up to 66% while the underestimations are  
498 much larger for the urban  $PM_{10}$  concentrations (up to 75%), suggesting that the urban  
499 emissions were not able to represent the actual emissions. The results show a systematic  
500 underestimation for all models in almost all seasons and sub-regions, with the largest  
501 underestimations for the Mediterranean region. The results also show overestimations in  
502  $PM_{2.5}$  levels suggesting the large underestimations in the  $PM_{10}$  levels can be attributed to the



503 natural emissions. Over NA, there are no systematic seasonal trends in model performances  
504 except for the ES1 and US8 models having the largest biases for rural PM<sub>10</sub> levels in all  
505 seasons and sub-regions. There is a general underestimation in all seasons and sub-regions,  
506 with the exception of overestimations calculated for US7 model by 3% to 67% over western  
507 US. The highest underestimations were calculated for the spring and summer periods in all  
508 sub-regions by up to ~90%. In general, majority of the models simulating the NA case have  
509 smaller biases compared to those simulating the EU case, in particular regarding PM<sub>2.5</sub>, which  
510 suggests a better representation of the anthropogenic emissions in NA.

511 SO<sub>4</sub> levels over EU are underestimated by majority of the models by up to 61% while few  
512 groups overestimated the SO<sub>4</sub> levels by 7% to 52%. NO<sub>3</sub> levels are overestimated by majority  
513 of the models in all regions by more than 75%, particularly in east and south Europe while  
514 NH<sub>4</sub> levels are also underestimated largely in south Europe. SO<sub>4</sub> levels over NA are  
515 particularly overestimated over western US that is characterized by large anthropogenic  
516 emissions. Eastern US is characterized by underestimated SO<sub>4</sub> levels by the majority of the  
517 models. Regarding the AOD<sub>555</sub>, the majority of the model performed within the 50% error  
518 range over EU. Differences in models can be attributed to differences in approaches in  
519 estimating the AOD such as the aerosol components considered in these estimations. The  
520 observed hourly diurnal variation over the continent was moderately captured by the models  
521 while WRF/CHEM models were associated with very similar temporal variations. Over NA,  
522 the CA2f and US7 models overestimate the observed AOD<sub>555</sub> levels by up to 29% while the  
523 US6 and US8 models underestimate by up to 32%. Results show that the simulated dry  
524 deposition simulated can lead to substantial differences among the models.

525 Overall, the results show that representation of dust and sea-salt emissions can largely impact  
526 the simulated PM concentrations and that there are still major challenges and uncertainties in  
527 simulating the PM levels and identifying the source of the bias in the models. It should be  
528 noted that as the results presented in this paper are temporally and spatially averaged over the  
529 seasons and sub-regions, cases where feedback mechanisms are of importance must be further  
530 studied and evaluated in order to better evaluate the skills of these models in simulating the  
531 feedback mechanisms and their impact on the surface PM levels.

532

### 533 Acknowledgements

534 We gratefully acknowledge the contribution of various groups to the second air Quality  
535 Model Evaluation international Initiative (AQMEII) activity: U.S. EPA, Environment Canada,  
536 Mexican Secretariat of the Environment and Natural Resources (Secretaría de Medio  
537 Ambiente y Recursos Naturales-SEMARNAT) and National Institute of Ecology (Instituto  
538 Nacional de Ecología-INE) (North American national emissions inventories); U.S. EPA  
539 (North American emissions processing); TNO (European emissions processing);  
540 ECMWF/MACC project & Météo-France/CNRM-GAME (Chemical boundary conditions).  
541 Ambient North American concentration measurements were extracted from Environment  
542 Canada's National Atmospheric Chemistry Database (NAtChem) PM database and provided  
543 by several U.S. and Canadian agencies (AQS, CAPMoN, CASTNet, IMPROVE, NAPS,

544 SEARCH and STN networks); North American precipitation-chemistry measurements were  
545 extracted from NAtChem's precipitation-chemistry data base and were provided by several  
546 U.S. and Canadian agencies (CAPMoN, NADP, NBPMN, NSPSN, and REPQ networks); the  
547 WMO World Ozone and Ultraviolet Data Centre (WOUDC) and its data-contributing  
548 agencies provided North American and European ozonesonde profiles; NASA's AErosol  
549 RObotic NETwork (AeroNet) and its data-contributing agencies provided North American  
550 and European AOD measurements; the MOZAIC Data Centre and its contributing airlines  
551 provided North American and European aircraft takeoff and landing vertical profiles; for  
552 European air quality data the following data centers were used: EMEP European Environment  
553 Agency/European Topic Center on Air and Climate Change/AirBase provided European air-  
554 and precipitation-chemistry data. The Finish Meteorological Institute is acknowledged for  
555 providing biomass burning emission data for Europe. Data from meteorological station  
556 monitoring networks were provided by NOAA and Environment Canada (for the US and  
557 Canadian meteorological network data) and the National Center for Atmospheric Research  
558 (NCAR) data support section. Joint Research Center Ispra/Institute for Environment and  
559 Sustainability provided its ENSEMBLE system for model output harmonization and analyses  
560 and evaluation. The co-ordination and support of the European contribution through COST  
561 Action ES1004 EuMetChem is gratefully acknowledged. The views expressed here are those  
562 of the authors and do not necessarily reflect the views and policies of the U.S. Environmental  
563 Protection Agency (EPA) or any other organization participating in the AQMEII project. This  
564 paper has been subjected to EPA review and approved for publication. C. Knote was  
565 supported by the DOE grant DE-SC0006711. The UPM authors thankfully acknowledge the  
566 computer resources, technical expertise and assistance provided by the Centro de  
567 Supercomputación y Visualización de Madrid (CESVIMA) and the Spanish Supercomputing  
568 Network (BSC). G. Curci and P. Tuccella were supported by the Italian Space Agency (ASI)  
569 in the frame of PRIMES project (contract n.I/017/11/0). The Centre of Excellence for Space  
570 Sciences and Technologies SPACE-SI is an operation partly financed by the European Union,  
571 European Regional Development Fund and Republic of Slovenia, Ministry of Higher  
572 Education, Science, Sport and Culture. Y. Zhang acknowledges funding support from the NSF  
573 Earth System Program (AGS-1049200) and high-performance computing support from  
574 Yellowstone by NCAR's Computational and Information Systems Laboratory, sponsored by  
575 the National Science Foundation and Stampede, provided as an Extreme Science and  
576 Engineering Discovery Environment (XSEDE) digital service by the Texas Advanced  
577 Computing Center (TACC). The technical assistance of Bert van Uft (KNMI) and Arjo  
578 Segers (TNO) in producing the results of the RACMO2-LOTOS-EUROS system is gratefully  
579 acknowledged. L. Giordano was supported by the Swiss SERI COST project C11.0144. UH-  
580 CAIR acknowledges support from the TRANSPHORM (FP7) project which provided the  
581 basis for their modelling approaches.

582

583 REFERENCES

584

- 585 Ahmadov, R., McKeen, S. A., Robinson, A., Bahreini, R., Middlebrook, A., de Gouw, J.,  
586 Meagher, J., Hsie, E., Edgerton, E., Shaw, S., Trainer, M., 2012. A volatility basis set model  
587 for summertime secondary organic aerosols over the eastern United States in 2006. *Journal of*  
588 *Geophysical Research*, 117, D06301.
- 589  
590 Ackermann, I.J., Hass, H., Memmesheimer, M., Ebel, A., Binkowski, F.S., Shankar, U., 1998.  
591 Modal aerosol dynamics model for Europe: Development and first applications. *Atmospheric*  
592 *Environment*, 32, 17, 2981-2999.
- 593  
594 Appel, K. W., Pouliot, G. A., Simon, H., Sarwar, G., Pye, H. O. T., Napelenok, S. L., Akhtar,  
595 F., Roselle, S. J., 2013. Evaluation of dust and trace metal estimates from the Community  
596 Multiscale Air Quality (CMAQ) model version 5.0. *Geoscientific Model Development*, 6,  
597 883-899.
- 598  
599 Appel, K.W., Bhave, P.V., Gilliland, A.B., Sarwar, G., Roselle, S.J., 2008. Evaluation of the  
600 community multiscale air quality (CMAQ) model version 4.5: Sensitivities impacting model  
601 performance; Part II particulate matter. *Atmospheric Environment*, 42, 6057– 6066.
- 602  
603 Baklanov, A., Schlünzen, K., Suppan, P., Baldasano, J., Brunner, D., Aksoyoglu, S.,  
604 Carmichael, G., Douros, J., Flemming, J., Forkel, R., Galmarini, S., Gauss, M., Grell, G.,  
605 Hirtl, M., Joffre, S., Jorba, O., Kaas, E., Kaasik, M., Kallos, G., Kong, X., Korsholm, U.,  
606 Kurganskiy, A., Kushta, J., Lohmann, U., Mahura, A., Manders-Groot, A., Maurizi, A.,  
607 Moussiopoulos, N., Rao, S. T., Savage, N., Seigneur, C., Sokhi, R. S., Solazzo, E.,  
608 Solomos, S., Sørensen, B., Tsegas, G., Vignati, E., Vogel, B., Zhang, Y., 2014. Online  
609 coupled regional meteorology chemistry models in Europe: current status and prospects.  
610 *Atmospheric Chemistry and Physics*, 14, 317-398.
- 611  
612 Balzarini, A., Pirovano, G., Honzak, L., Zabkar, R., Curci, G., Forkel, R., Hirtl, M., San José,  
613 R., Tuccella, P., Grell, G.A., 2014. WRF-Chem model sensitivity to chemical mechanism  
614 choice in reconstructing aerosol optical properties. *Atmospheric Environment*, Submitted.
- 615  
616 Bellouin, N., Rae, J., Jones, A., Johnson, C., Haywood, J., Boucher, O., 2011. Aerosol forcing  
617 in the Climate Model Intercomparison Project (CMIP5) simulations by HadGEM2-ES and the  
618 role of ammonium nitrate. *Journal of Geophysical Research-Atmosphere*, 116, D20206.
- 619  
620 Beltman, J.B., Hendriks, C., Tum, M., Schaap, M., 2013. The impact of large scale biomass  
621 production on ozone air pollution in Europe. *Atmospheric Environment*, 71, 352-363.
- 622  
623 Bernard, S.M., Samet, J.M., Grambsch, A., Ebi, K.L., Romieu, I., 2001. The potential  
624 impact of climate variability and change on air pollution-related health effects in  
625 the United States. *Environmental Health Perspectives* 109 (Suppl. 2), 199-209.
- 626  
627 Bianconi, R., Galmarini, S., Bellasio, R., 2004. Web-based system for decision support  
628 in case of emergency: ensemble modelling of long-range atmospheric dispersion  
629 of radionuclides. *Environmental Modelling and Software* 19, 401-411.
- 630  
631 Brunner, D., Jorba, O., Savage, N., Eder, B., Makar, P., Giordano, L., Badia, A., Balzarini, A.,  
632 Baro, R., Bianconi, R., Chemel, C., Forkel, R., Jimenez-Guerrero, P., Hirtl, M., Hodzic, A.,  
633 Honzak, L., Im, U., Knote, C., Kuenen, J.J.P., Makar, P.A., Manders-Groot, A., Neal, L.,  
634 Perez, J.L., Pirovano, G., San Jose, R., Savage, N., Schroder, W., Sokhi, R.S., Syrakov, D.,

- 635 Torian, A., Werhahn, K., Wolke, R., van Meijgaard, E., Yahya, K., Zabkar, R., Zhang, Y.,  
636 Zhang, J., Hogrefe, C., Galmarini, S., 2014. Evaluation of the meteorological performance of  
637 coupled chemistry-meteorology models in phase 2 of the Air Quality Model Evaluation  
638 International Initiative. *Atmospheric Environment*, to be submitted.
- 639  
640 Curci, G., Balzarini, A., Baró, R., Bianconi, R., Brunner, D., Forkel, R., Giordano, L., Hirtl,  
641 M., Hogrefe, C., Honzak, L., Im, U., Jiménez-Guerrero, P., Knote, C., Langer, M., Makar, P.,  
642 Pirovano, G., Pérez, J.L., San José, R., Syrakov, D., Tuccella, P., Werhahn, J., Wolke, R.,  
643 Žabkar, R., 2014. Uncertainties of simulated aerosol optical properties induced by  
644 assumptions on aerosol physical and chemical properties, *Atmospheric Environment*,  
645 Submitted.
- 646  
647 Fountoukis, C., Nenes, A., 2007. ISORROPIA II: a computationally efficient thermodynamic  
648 equilibrium model for  $K^+ - Ca^{2+} - Mg^{2+} - NH_4^+ - Na^+ - SO_4^{2-} - NO_3^- - Cl^- - H_2O$  aerosols.  
649 *Atmospheric Chemistry and Physics*, 7, 4639-4659.
- 650  
651 Galmarini, S., Rao, S.T., 2011. The AQMEII two-continent Regional Air Quality Model  
652 evaluation study: Fueling ideas with unprecedented data. *Atmospheric Environment*, 45,  
653 2464.
- 654  
655 Galmarini, S., Bianconi, R., Appel, W., Solazzo, E., et al., 2012. ENSEMBLE and AMET:  
656 two systems and approaches to a harmonised, simplified and efficient assistance  
657 to air quality model developments and evaluation. *Atmospheric Environment*, 53, 51-59.
- 658  
659 Gong, S.L., Barrie, L.A., Blanchet, J.-P., von Salzen, K., Lohmann, U., Lesins, G., Spacek, L.,  
660 Zhang, L.M., Girard, E., Lin, H., Leaitch, R., Leighton, H., Chylek, P., Huang, P., 2003b.  
661 Canadian Aerosol Module: A size-segregated simulation of atmospheric aerosol processes for  
662 climate and air quality models 1. Module development. *Journal of Geophysical Research:*  
663 *Atmospheres*, 108, D01, AAC 3-1 – AAC 3-16.
- 664  
665 Gong, S.L., 2003. A parameterization of sea-salt aerosol source function for sub- and  
666 super-micron particles. *Global Biogeochemical Cycles* 17 (4), 1097.
- 667  
668 Gong, S.L., Barrie, L.A., Blanchet, J.-P., 1997. Modeling sea-salt aerosols in the atmosphere  
669 1. Model development. *Journal of Geophysical Research*, 102 (D3), 3805-3818.
- 670  
671 Grell, G.A. Baklanov, A., 2011. Integrated modelling for forecasting weather and air quality:  
672 a call for fully coupled approaches. *Atmospheric Environment*, 45, 6845–6851.
- 673  
674 Grell, G.A., Peckham, S.E., Schmitz, R., McKeen, S.A., Frost, G., Skamarock, W.C., Eder,  
675 B., 2005. Fully coupled “online” chemistry within the WRF model. *Atmospheric*  
676 *Environment*, 39, 6957-6975.
- 677  
678 Guenther, A., Karl, T., Harley, P., Wiedinmyer, C., Palmer, P.I., Geron, C., 2006. Estimates  
679 of global terrestrial isoprene emissions using MEGAN (Model of Emissions of Gases and  
680 Aerosols from Nature). *Atmospheric Chemistry and Physics*, 6, 3181-3210.
- 681  
682 Guenther, A.B., Zimmerman, P.R., Harley, P.C., Monson, R.K., Fall, R., 1993. Isoprene and  
683 monoterpene rate variability: model evaluations and sensitivity analyses. *Journal of*  
684 *Geophysical Research*, 98, D7, 12609-12617.

- 685  
686 Hogrefe, C., Roselle, S., Mathur, R., Rao, S.T., Galmarini, S., 2014. Space-time analysis of  
687 the Air Quality Model Evaluation International Initiative (AQMEII) Phase 1 air quality  
688 simulations. *Journal of Air Waste Management Association*, 64, 388-405.
- 689 Im, U., Bianconi, R., Solazzo, E., Kioutsioukis, I., Badia, A., Balzarini, A., Baró, R., Bellasio,  
690 R., Brunner, D., Chemel, C., Curci, G., Flemming, J., Forkel, R., Giordano, L., Jimenez-  
691 Guerrero, P., Hirtl, M., Hodzic, A., Honzak, L., Jorba, O., Knote, C., Kuenen, J.J.P., Makar,  
692 P.A., Manders-Groot, A., Neal, L., Perez, J.L., Pirovano, G., Pouliot, G., San Jose, R.,  
693 Savage, N., Schroder, W., Sokhi, R.S., Syrakov, D., Torian, A., Tuccella, P., Werhahn, K.,  
694 Wolke, R., Yahya, K., Zabkar, R., Zhang, Y., Zhang, J., Hogrefe, C., Galmarini, S., 2014.  
695 Evaluation of operational online-coupled regional air quality models over Europe and North  
696 America in the context of AQMEII phase 2. Part I: Ozone. *Atmospheric Environment*,  
697 Submitted.
- 698  
699 Inness, A., Baier, F., Benedetti, A., Bouarar, I., Chabrillat, S., Clark, H., Clerbaux, C.,  
700 Coheur, P., Engelen, R. J., Errera, Q., Flemming, J., George, M., Granier, C., Hadji-Lazaro, J.,  
701 Huijnen, V., Hurtmans, D., Jones, L., Kaiser, J. W., Kapsomenakis, J., Lefever, K., Leitão, J.,  
702 Razinger, M., Richter, A., Schultz, M. G., Simmons, A. J., Suttie, M., Stein, O., Thépaut, J.-  
703 N., Thouret, V., Vrekoussis, M., Zerefos, C., and the MACC team, 2013. The MACC  
704 reanalysis: an 8 yr data set of atmospheric composition. *Atmospheric Chemistry and Physics*,  
705 13, 4073-4109.
- 706  
707 IPCC: Climate change, 2007. Synthesis Report, Intergovernmental Panel on Climate  
708 Change.
- 709  
710 Jacob, D.J., Winner, D.A., 2009. Effect of climate change on air quality. *Atmospheric*  
711 *Environment* 41, 51-63.
- 712  
713 Jones, S., Creighton, G., 2011. AFWA dust emission scheme for WRF/Chem-GOCART.  
714 2011 WRF workshop, June 20-24, Boulder, CO, USA.
- 715  
716 Kelly, J.T., Bhave, P.V., Nolte, C.G., Shankar, U., Foley, K.M., 2010. Simulating emissions  
717 and chemical evolution of coarse sea-salt particles in the Community Multiscale Air Quality  
718 (CMAQ) model. *Geoscientific Model Development* 3, 257-273.
- 719  
720 Kioutsioukis, I., Im, U., Bianconi, R., Badia, A., Balzarini, A., Baró, R., Bellasio, R., Brunner,  
721 D., Chemel, C., Curci, G., Denier van der Gon, H., Flemming, J., Forkel, R., Giordano, L.,  
722 Jiménez-Guerrero, P., Hirtl, M., Jorba, O., Manders-Groot, A., Neal, L., Pérez, J.L., Piravano,  
723 G., San Jose, R., Savage, N., Schroder, W., Sokhi, R.S., Solazzo, E., Syrakov, D., Tuccella,  
724 P., Werhahn, J., Wolke, R., Hogrefe, C., Galmarini, S., 2014. Challenges in the deterministic  
725 skill of air quality ensembles. *Atmospheric Environment*, Submitted.
- 726  
727 Kuenen, J.J.P., Visschedijk, A.J.H., Jozwicka, M., Denier van der Gon, H.A.C., 2014.  
728 TNO\_MACC\_II emission inventory: a multi-year (2003-2009) consistent high-resolution  
729 European emission inventory for air quality modelling. *Atmospheric Chemistry and Physics*  
730 *Discussions*, 14, 5837-5869.
- 731  
732 Kulmala, M., Asmi, A., Lappalainen, H. K., Baltensperger, U., Brenguier, J.-L., Facchini, M.  
733 C., Hansson, H.-C., Hov, Ø., O'Dowd, C. D., Pöschl, U., Wiedensohler, A., Boers, R.,



- 734 Boucher, O., de Leeuw, G., Denier van der Gon, H. A. C., Feichter, J., Krejci, R., Laj, P.,  
735 Lihavainen, H., Lohmann, U., McFiggans, G., Mentel, T., Pilinis, C., Riipinen, I., Schulz, M.,  
736 Stohl, A., Swietlicki, E., Vignati, E., Alves, C., Amann, M., Ammann, M., Arabas, S., Artaxo,  
737 P., Baars, H., Beddows, D. C. S., Bergström, R., Beukes, J. P., Bilde, M., Burkhardt, J. F.,  
738 Canonaco, F., Clegg, S. L., Coe, H., Crumeyrolle, S., D'Anna, B., Decesari, S., Gilardoni, S.,  
739 Fischer, M., Fjaeraa, A. M., Fountoukis, C., George, C., Gomes, L., Halloran, P., Hamburger,  
740 T., Harrison, R. M., Herrmann, H., Hoffmann, T., Hoose, C., Hu, M., Hyvärinen, A., Hörrak,  
741 U., Iinuma, Y., Iversen, T., Josipovic, M., Kanakidou, M., Kiendler-Scharr, A., Kirkevåg, A.,  
742 Kiss, G., Klimont, Z., Kolmonen, P., Komppula, M., Kristjánsson, J.-E., Laakso, L.,  
743 Laaksonen, A., Labonnote, L., Lanz, V. A., Lehtinen, K. E. J., Rizzo, L. V., Makkonen, R.,  
744 Manninen, H. E., McMeeking, G., Merikanto, J., Minikin, A., Mirme, S., Morgan, W. T.,  
745 Nemitz, E., O'Donnell, D., Panwar, T. S., Pawlowska, H., Petzold, A., Pienaar, J. J., Pio, C.,  
746 Plass-Duelmer, C., Prévôt, A. S. H., Pryor, S., Reddington, C. L., Roberts, G., Rosenfeld, D.,  
747 Schwarz, J., Seland, Ø., Sellegri, K., Shen, X. J., Shiraiwa, M., Siebert, H., Sierau, B.,  
748 Simpson, D., Sun, J. Y., Topping, D., Tunved, P., Vaattovaara, P., Vakkari, V., Veeffkind, J.  
749 P., Visschedijk, A., Vuollekoski, H., Vuolo, R., Wehner, B., Wildt, J., Woodward, S.,  
750 Worsnop, D. R., van Zadelhoff, G.-J., Zardini, A. A., Zhang, K., van Zyl, P. G., Kerminen,  
751 V.-M., S Carslaw, K., Pandis, S. N., 2011. General overview: European Integrated project on  
752 Aerosol Cloud Climate and Air Quality interactions (EUCAARI) – integrating aerosol  
753 research from nano to global scales. *Atmospheric Chemistry and Physics*, 11, 13061-13143.  
754
- 755 Long M.S., Keene W.D., Kieber D.J., Erickson D.J., Maring H., 2011. A sea-state based  
756 source function for size- and composition-resolved marine aerosol production. *Atmospheric*  
757 *Chemistry and Physics*, 11, 1203-1216.  
758
- 759 Lundgren, K., 2006. Numerical simulation of the spatial and temporal distribution of sea salt  
760 particles on the regional scale. M. Sc. thesis, Department of Meteorology Stockholm  
761 University, Stockholm, Sweden, 2006.  
762
- 763 Makar, P.A., Gong, W., Hogrefe, C., Zhang, Y., Curci, G., Zabkar, R., Milbrandt, J., Im, U.,  
764 Galmarini, S., Balzarini A., Baro, R., Bianconi, R., Cheung, P., Forkel, R., Gravel, S., Hirtl,  
765 M., Honzak, L., Hou, A., Jimenez-Guerrero, P., Langer M., Moran, M.D., Pabla, B., Perez,  
766 P.L., Pirovano, G., San Jose, R., Tuccella, P., Werhahn, J., Zhang, J., 2014a. Feedbacks  
767 between Air Pollution and Weather, Part 1: Effects on Chemistry. *Atmospheric Environment*,  
768 Submitted.  
769
- 770 Makar, P.A., Gong, W., Hogrefe, C., Zhang, Y., Curci, G., Zabkar, R., Milbrandt, J., Im, U.,  
771 Galmarini, S., Balzarini A., Baro, R., Bianconi, R., Cheung, P., Forkel, R., Gravel, S., Hirtl,  
772 M., Honzak, L., Hou, A., Jimenez-Guerrero, P., Langer M., Moran, M.D., Pabla, B., Perez,  
773 P.L., Pirovano, G., San Jose, R., Tuccella, P., Werhahn, J., Zhang, J., 2014b. Feedbacks  
774 between Air Pollution and Weather, Part 2: Effects on Weather. *Atmospheric Environment*,  
775 Submitted.  
776
- 777 Mansell, G.E., Lau, S., Russel, J., Omary, M., 2006. Final report: Fugitive wind blown dust  
778 emissions and model performance evaluation: Phase II. Report prepared for Western  
779 Governors Association. Novato, Cal.: Environ International Corp.  
780
- 781 Pouliot, G., Denier van der Gon, H., Kuenen, J., Makar, P., Zhang, J., Moran, M., 2014.  
782 Analysis of the Emission Inventories and Model-Ready Emission Datasets of Europe and  
783 North America for Phase 2 of the AQMEII Project. *Atmospheric Environment*, Submitted.



- 784  
785 Raman, A., Arellano, A., 2013. Modeling and Data Analysis of 2011 Phoenix Dust Storm.  
786 oral presentation at the 15<sup>th</sup> Conference on Atmospheric Chemistry/93<sup>rd</sup> AMS annual meeting,  
787 Austin, Texas, U.S.A., 6-10 January.  
788
- 789 Riemer, N., Vogel, H., Vogel, B., Fiedler, F., 2003. Modeling aerosols on the mesoscale- $\gamma$ :  
790 Treatment of soot aerosol and its radiative effects. *Journal of Geophysical Research*, 108: doi:  
791 10.1029/2003JD003448. issn: 0148-0227.  
792
- 793 Savage, N. H., Agnew, P., Davis, L. S., Ordóñez, C., Thorpe, R., Johnson, C. E., O'Connor, F.  
794 M., Dalvi, M., 2013. Air quality modelling using the Met Office Unified Model (AQUUM  
795 OS24-26): model description and initial evaluation. *Geoscientific Model Development*, 6,  
796 353-372.  
797
- 798 Schaap, M., Manders, A. M. M., Hendriks, E. C. J., Cnossen, J. M., Segers, A. J. S., Denier  
799 van der Gon, H. A. C., Jozwicka, M., Sauter, F., Velders, G., Matthijsen, J., Bultjes, P. J. H.,  
800 2009. Regional modelling of particulate matter for the Netherlands. PBL Report 500099008,  
801 Netherlands Environmental Assessment Agency, AH Bilthoven, the Netherlands, 2009.  
802
- 803 Schaap, M., M. Roemer, F. Sauter, G. Boersen, R. Timmermans, P.J.H. Bultjes, 2005.  
804 LOTOS-EUROS: Documentation, TNO report B&O-A, 2005-297, Apeldoorn, 2005.  
805
- 806 Shaw, W.J., Allwine, K.J., Fritz, B.G., Rutz, F.C., Rishel, J.P., Chapman, E.G., 2008. An  
807 evaluation of the wind erosion module in DUSTAN. *Atmospheric Environment*, 42, 1907-  
808 1921.  
809
- 810 Schell B., Ackermann, I. J., Hass, H., Binkowski, F.S., Ebel, A., 2001. Modeling the  
811 formation of secondary organic aerosol within a comprehensive air quality model system.  
812 *Journal of Geophysical Research*, 106, 28275-28293.  
813
- 814 Schere, K., Flemming, J., Vautard, R., Chemel, C., Colette, A., Hogrefe, C., Bessagnet, B.,  
815 Meleux, F., Mathur, R., Roselle, S., Hu, R.-M., Sokhi, R. S., Rao, S.T., S. Galmarini, 2012:  
816 Trace gas/aerosol boundary concentrations and their impacts on continental-scale AQMEII  
817 modeling domains, *Atmospheric Environment*, 53, 38-50.  
818
- 819 Schwartz, J., Dockery, D.W., Neas, L.M., 1996. Is daily mortality associated specifically  
820 with fine particles? *Journal of Air and Waste Management Association* 46,  
821 927-939.  
822
- 823 Schwede, D., Pouliot, G., Pierce, T., 2005. Changes to the Biogenic Emissions Inventory  
824 System version 3 (BEIS3). In: 4th CMAS Models-3 Users' Conference, Chapel Hill, NC, 26-  
825 28 September 2005.  
826
- 827 Soares, J., Sofiev, M., Prank, M., San Jose, R., Perez, J.L., 2014. On uncertainties of wild-land  
828 fires emission in AQMEII case study. *Atmospheric Environment*, In preparation.  
829
- 830 Sofiev, M., Vankevich, R., Lotjonen, M., Prank, M., Petukhov, V., Ermakova, T., Koskinen,  
831 J., Kukkonen, J., 2009. An operational system for the assimilation of the satellite information  
832 on wild-land fires for the needs of air quality modelling and forecasting. *Atmospheric  
833 Chemistry and Physics*, 9, 6833-6847.

- 834  
835 Solazzo, E., Bianconi, R., Pirovano, G., Moran, M., Vautard, R., Hogrefe, C., Appel, K.W.,  
836 Matthias, V., Grossi, P., Bessagnet, B., Brandt, J., Chemel, C., Christensen, J.H., Forkel, R.,  
837 Francis, X.V., Hansen, A., McKeen, S., Nopmongcol, U., Prank, M., Sartelet, K.N., Segers,  
838 A., Silver, J.D., Yarwood, G., Werhahn, J., Zhang, J., Rao, S.T., Galmarini, S. 2013.  
839 Evaluating the capabilities of regional scale air quality models to capture the vertical  
840 distribution of pollutants. *Geoscientific Model Development* 6, 791-818, 2013.  
841  
842 Solazzo, E., Bianconi, R., Vautard, R., Appel, K. W., Moran, M. D., Hogrefe, C., Bessagnet,  
843 B., Brandt, J., Christensen, J. H., Chemel, C., Coll, I., van der Gon, H. D., Ferreira, J.,  
844 Forkel, R., Francis, X. V., Grell, G., Grossi, P., Hansen, A. B., Jericevic, A., Kraljevic, L.,  
845 Miranda, A. I., Nopmongcol, U., Pirovano, G., Prank, M., Riccio, A., Sartelet, K. N., Schaap,  
846 M., Silver, J. D., Sokhi, R. S., Vira, J., Werhahn, J., Wolke, R., Yarwood, G., Zhang, J., Rao,  
847 S. T., Galmarini, S., 2012a. Ensemble modelling of surface level ozone in Europe and North  
848 America in the context of AQMEI. *Atmospheric Environment*, 53, 60–74.  
849  
850 Solazzo, E., Bianconi, R., Pirovano, G., Matthias, V., Vautard, R., Moran, M. D., Appel, K.  
851 W., Bessagnet, B., Brandt, J., Christensen, J. H., Chemel, C., Coll, I., Ferreira, J., Forkel, R.,  
852 Francis, X. V., Grell, G., Grossi, P., Hansen, A. B., Hogrefe, C., Miranda, A. I., Nopmongco,  
853 U., Prank, M., Sartelet, K. N., Schaap, M., Silver, J. D., Sokhi, R. S., Vira, J., Werhahn, J.,  
854 Wolke, R., Yarwood, G., Zhang, J., Rao, S. T., Galmarini, S., 2012b. Operational model  
855 evaluation for particulate matter in Europe and North America in the context of AQMEI.  
856 *Atmospheric Environment*, 53, 75–92.  
857  
858 Tegen, I., Harrison, S.P., Kohfeld, K.E., Prentice, I.C., Coe, M.C., Heimann, M., 2002. The  
859 impact of vegetation and preferential source areas on global dust aerosol: results from a model  
860 study. *Journal of Geophysical Research* 107, doi:10.1029/2001JD000963  
861  
862 Vautard, R., Moran, M. D., Solazzo, E., Gilliam, R. C., Matthias, V., Bianconi, R., Chemel,  
863 C., Ferreira, J., Geyer, B., Hansen, A. B., Jericevic, A., Prank, M., Segers, A., Silver, J. D.,  
864 Werhahn, J., Wolke, R., Rao, S. T., and Galmarini, S.: Evaluation of the meteorological  
865 forcing used for AQMEI air quality simulations, *Atmos. Environ.*, 53, 15–37, 2012.  
866  
867 Vogel, B., Vogel, H., Baumer, D., Bangert, M., Lundgren, K., Rinke, R., Stanelle, T., 2009.  
868 The comprehensive model system COSMO-ART – Radiative impact of aerosol on the state of  
869 the atmosphere on the regional scale. *Atmospheric Chemistry and Physics*, 9, 8661–  
870 8680.  
871  
872 Wang, K., Yahya, K., Zhang, Y., Wu, S.-Y., Grell, G., 2014. Implementation and Initial  
873 Application of A New Chemistry-Aerosol Option in WRF/Chem for Simulation of Secondary  
874 Organic Aerosols and Aerosol Indirect Effects. *Atmospheric Environment*, in review.  
875  
876 Winker, D.M., Tackett, J.L., Getzewich, B.J., Liu, Z., Vaughan, V.A., Rogers, R.R., 2013.  
877 The global 3-D distribution of tropospheric aerosols as characterized by CALIOP.  
878 *Atmospheric Chemistry and Physics*, 13, 3345-3361.  
879  
880 Wolke, R., Schroder, W., Schrodner, R., Renner, E., 2012. Influence of grid resolution and  
881 meteorological forcing on simulated European air quality: a sensitivity study with the  
882 modeling system COSMO–MUSCAT. *Atmospheric Environment* 53, 110–130.  
883

- 884 Wong, D. C., Pleim, J., Mathur, R., Binkowski, F., Otte, T., Gilliam, R., Pouliot, G., Xiu, A.,  
885 Young, J. O., Kang, D., 2012. WRF-CMAQ two-way coupled system with aerosol feedback:  
886 software development and preliminary results. *Geoscientific Model Development*, 5, 299-312.  
887
- 888 Yahya, K., Wang, K., Zhang, Y., Kleindienst, T. E., 2014a. Application of WRF/Chem over  
889 North America under the AQMEII Phase II. Part II. Comprehensive Evaluation of 2010  
890 Simulation and Responses of Air Quality and Meteorology-Chemistry Interactions to Changes  
891 in Emissions and Meteorology from 2006 to 2010. *Atmospheric Environment*, in preparation.  
892
- 893 Yahya, K., Wang, K., Gudoshava, M., Glotfelty, T., Zhang, Y., 2014b. Application of  
894 WRF/Chem over North America under the AQMEII Phase II. Part I. Comprehensive  
895 Evaluation of 2006 Simulation. *Atmospheric Environment*, in review.  
896
- 897 Zaveri, R.A., Easter, R.C., Fast, J.D., Peters, L.K., 2008. Model for simulating aerosol  
898 interactions and chemistry (MOSAIC). *Journal of Geophysical Research*, 113, D13204.  
899
- 900 Zhang, Y., 2008. Online-coupled meteorology and chemistry models: history, current status,  
901 and outlook. *Atmospheric Chemistry and Physics*, 8, 2895–2932.  
902
- 903 Zhao, C., Liu, X., Leung, L. R., Johnson, B., McFarlane, S. A., Gustafson Jr., W. I., Fast, J.  
904 D., Easter, R., 2010. The spatial distribution of mineral dust and its shortwave radiative  
905 forcing over North Africa: modeling sensitivities to dust emissions and aerosol size  
906 treatments. *Atmospheric Chemistry and Physics*, 10, 8821-8838.

Table 1. Model groups participated to AQMEII2

No	Acronym	Domain	Model	Resolution	Biogenic Model	Dust Model	Sea-salt Model	Aerosol	Reference
1	AT1	EU	WRF/Chem	23 km	MEGAN <sup>1</sup>	MOSAIC <sup>3</sup> MADE <sup>4</sup> /SORGAM <sup>5</sup>	MOSAIC MADE/SORGAM	MADE/SORGAM	Grell et al., 2005
2	BG2	EU	WRF-CMAQ	25 km	BEIS <sup>2</sup>	Mansell et al., 2006	AERO4 <sup>9</sup>	AERO4	Appel et al., 2008
3	CH1	EU	COSMO-ART	0.22 °	Gunter et al., 1998	Vogel et al., 2006	Lundgren, 2006	MADEsoot <sup>10</sup>	Vogel et al., 2009
4	DE3	EU	COSMO-MUSCAT	0.25 °	Gunther et al., 1993	Tegen et al., 2002	Long et al., 2011	Simpson et al., 2003	Wolke et al., 2012
5	DE4	EU	WRF/Chem	23 km	MEGAN	MOSAIC MADE/SORGAM	MOSAIC MADE/SORGAM	MADE/SORGAM	Grell et al., 2005
6	ES1	EU	WRF/Chem	23 km	MEGAN	MOSAIC MADE/SORGAM	MOSAIC MADE/SORGAM	MADE/SORGAM	Grell et al., 2005
7	ES3	EU	WRF/Chem	23 km	MEGAN	N/A	MOSAIC MADE/SORGAM	MOSAIC 4 bins	Grell et al., 2005
8	IT1	EU	WRF/Chem	23 km	MEGAN	MOSAIC MADE/SORGAM	MOSAIC MADE/SORGAM	MADE/SORGAM	Grell et al., 2005
9	IT2	EU	WRF/Chem	23 km	MEGAN	DUSTRUN <sup>6</sup>	MOSAIC MADE/SORGAM	MADE/VBS <sup>11</sup>	Grell et al., 2005
10	NL2	EU	RACMO LOTOS-EUROS	0.5°×0.25°	Beltman et al., 2013	Schaap et al., 2009	Schaap et al., 2009	ISORRAPIA II 2 bins <sup>12</sup>	Sauter et al., 2012
11	SI1	EU	WRF/Chem	23 km	MEGAN	MOSIC MADE/SORGAM	MOSAIC MADE/SORGAM	MADE	Grell et al., 2005
12	UK4	EU	MetUM UKCA- RAQ	0.22 °	TNO	Woodward, 2001	N/A	Bellouin et al., 2011	Savage et al., 2013
13	UK5	EU	WRF-CMAQ	18 km	MEGAN	N/A	Kelly et al., 2010	AERO6 <sup>14</sup>	Wong et al., 2012
14	CA2f	NA	GEM-MACH	15 km	BEIS	N/A	Gong et al., 2003	CAM <sup>13</sup>	Makar et al., 2014a,b
15	ES1	NA	WRF/Chem	36 km	MEGAN	MOSAIC MADE/SORGAM	MOSAIC MADE/SORGAM	MADE/SORGAM	Grell et al., 2005
16	US6	NA	WRF-CMAQ	12 km	BEIS3.14	Appel et al., 2013	Kelly et al., 2010	AERO6	Wong et al., 2012
17	US7	NA	WRF/Chem	36 km	MEGAN	GOCART AFWA <sup>7</sup>	Gong et al., 1997	MOSAIC	Grell et al., 2005
18	US8	NA	WRF/Chem	36 km	MEGAN	AFWA/AER <sup>8</sup>	Gong et al., 1997	MADE/VBS	Grell et al., 2005

1. Guenther et al., 2006; 2. Schwede et al., 2005; 3. Zaveri et al., 2008; 4. Ackermann et al., 1998; 5. Schell et al., 2001; 6. Schaw et al., 2008; 7. Jones and Creighton, 2011; 8. XXX; 9. Appel et al., 2008; 10. Riemer et al., 2003; 11. Ahmadv et al., 2012; 12. Fountoukis and Nenes, 2007; 13. Gong et al., 2003b.14. Appel et al., 2013

Table 2. Statistical comparisons of observed and simulated annual and domain-mean surface PM<sub>10</sub> and PM<sub>2.5</sub> over EU and NA

Models	PM <sub>10</sub>								PM <sub>2.5</sub>							
	Rural				Urban				Rural				Urban			
	<i>r</i>	<i>NMSE</i> (%)	<i>NMB</i> (%)	<i>RMSE</i> ( $\mu\text{g m}^{-3}$ )	<i>r</i>	<i>NMSE</i> (%)	<i>NMB</i> (%)	<i>RMSE</i> ( $\mu\text{g m}^{-3}$ )	<i>r</i>	<i>NMSE</i> (%)	<i>NMB</i> (%)	<i>RMSE</i> ( $\mu\text{g m}^{-3}$ )	<i>r</i>	<i>NMSE</i> (%)	<i>NMB</i> (%)	<i>RMSE</i> ( $\mu\text{g m}^{-3}$ )
AT1	0.40	55.34	-43.55	11.06	0.34	125.19	-61.70	22.72	0.34	38.17	-31.67	6.91	0.38	72.32	-45.33	11.14
BG2	0.74	55.30	-46.86	10.72	0.76	141.76	-65.14	23.07	0.80	33.27	-36.58	6.22	0.84	62.53	-47.46	10.15
CH1	0.42	29.93	-28.52	9.17	0.27	85.20	-53.82	20.64	0.29	24.42	-1.28	6.67	0.34	34.71	-24.58	9.10
DE3	0.63	45.54	-41.88	10.18	0.58	130.79	-63.26	22.75	0.60	23.70	-24.82	5.71	0.67	49.99	-40.07	9.70
DE4	0.18	59.13	-43.64	11.42	0.06	125.63	-61.30	22.88	0.11	44.01	-31.74	7.42	0.08	82.12	-46.42	11.75
ES1	0.22	74.83	-49.19	12.20	0.16	152.22	-65.15	23.90	0.21	52.93	-38.19	7.74	0.22	94.45	-50.72	12.09
ES3	0.35	77.96	-50.74	12.26	0.11	182.13	-68.38	24.90	0.23	44.98	-34.03	7.37	0.28	81.27	-47.52	11.57
IT1	0.57	21.70	-25.12	7.97	0.47	68.83	-50.29	19.20	0.52	16.70	-12.28	5.18	0.56	35.91	-29.89	8.89
IT2	0.26	168.83	-66.10	14.97	0.25	270.45	-75.24	26.86	0.16	132.25	-59.65	9.89	0.23	209.61	-67.99	14.51
NL2	0.61	34.54	-35.68	9.32	0.57	97.69	-57.61	21.12	0.65	41.25	-37.94	6.85	0.75	81.28	-50.94	11.19
SI1	0.62	17.63	-21.52	7.36	0.57	62.11	-48.67	18.53	0.60	13.84	-9.33	4.80	0.60	30.67	-27.30	8.37
UK4	0.25	31.91	-23.29	9.79	0.07	53.46	-42.58	18.18	0.03	55.49	19.42	11.02	0.16	28.54	-8.34	9.06
UK5	0.86	50.34	-46.32	10.28	0.82	116.40	-61.83	21.88	0.84	48.04	-44.39	7.00	0.90	81.46	-53.39	10.92
EU Mean	0.64	43.49	-40.29	10.08	0.52	109.88	-59.55	21.88	0.49	28.54	-26.70	6.19	0.60	57.47	-41.61	10.26
EU Median	0.68	50.52	-43.50	10.57	0.56	124.21	-61.95	22.56	0.56	34.57	-32.37	6.55	0.64	68.40	-45.85	10.78
CA2f	-0.10	49.37	-19.79	15.64	0.33	5.40	-4.72	5.68	0.51	10.23	19.67	2.47	0.65	11.15	29.42	3.99
ES1	0.41	344.08	-76.91	22.15	0.16	363.46	-81.04	20.81	0.05	175.80	-67.97	5.29	0.24	250.59	-74.98	8.32
US6	0.21	63.65	-38.22	15.58	0.34	19.85	-31.43	9.25	0.41	11.07	-6.05	2.27	0.68	7.90	8.58	3.08
US7	0.20	34.17	-17.21	13.22	0.55	7.79	-18.06	6.33	0.61	20.84	46.89	3.90	0.56	16.15	36.11	4.93
US8	0.31	438.30	-80.09	23.22	0.49	216.12	-73.74	18.88	0.46	18.99	-25.49	2.65	0.62	13.81	-24.87	3.39
NA Mean	0.24	83.01	-46.45	16.57	0.60	33.85	-42.10	11.10	0.58	7.31	-6.78	1.84	0.74	3.54	-5.30	1.92
NA Median	0.18	115.82	-54.21	18.10	0.54	46.72	-47.43	12.42	0.55	9.19	-11.69	2.01	0.72	4.07	-6.48	2.05

## Figure Captions

**Fig.1.** Standard annual  $PM_{2.5}$  emissions in Europe and North America overlaid with monitoring stations in the sub-regions (upper panel: the red circles show EU1/NA1, yellow diamonds show EU2/NA2 and green squares show EU3/NA3) and monthly time series of anthropogenic  $PM_{2.5}$  emissions over EU and NA (lower panel). Note scale differences.

**Fig.2.** Observed and simulated monthly continental and sub-regional rural  $PM_{10}$  concentrations over EU (upper panel) and NA (lower panel). Note scale differences.

**Fig.3.** Observed and simulated monthly continental and sub-regional urban  $PM_{10}$  concentrations over EU (upper panel) and NA (lower panel). Note scale differences.

**Fig.4.** Box-and-whisker plots for observed and simulated  $PM_{10}$  (upper panel) and  $PM_{2.5}$  (lower panel) concentrations over rural and urban stations in Europe and North America.

**Fig.5.** Soccer plots for simulated seasonal and regional rural  $PM_{10}$  levels over Europe (upper panel) and North America (lower panel) for winter (a,e), spring (b,f), summer (c,g) and autumn (d,h).

**Fig.6.** Soccer plots for simulated seasonal and regional urban  $PM_{10}$  levels over Europe (upper panel) and North America (lower panel) for winter (a,e), spring (b,f), summer (c,g) and autumn (d,h).

**Fig.7.** Observed and simulated monthly continental and sub-regional rural  $PM_{2.5}$  concentrations over EU (upper panel) and NA (lower panel). Note scale differences.

**Fig.8.** Observed and simulated monthly continental and sub-regional urban  $PM_{2.5}$  concentrations over EU (upper panel) and NA (lower panel). Note scale differences.

**Fig.9.** Calculated annual dry deposition of fine inorganic aerosols ( $SO_4$ ,  $NO_3$  and  $NH_4$ ), total organic carbon (TOC)  $PM_{2.5}$ , crustal material (CM) and sea-salt (SS) over a,b) EU and c,d) NA.

**Fig.10.** Soccer plots for simulated seasonal and regional rural  $PM_{2.5}$  levels over Europe (upper panel) and North America (lower panel) for winter (a,e), spring (b,f), summer (c,g) and autumn (d,h).

**Fig.11.** Soccer plots for simulated seasonal and regional urban  $PM_{2.5}$  levels over Europe (upper panel) and North America (lower panel) for winter (a,e), spring (b,f), summer (c,g) and autumn (d,h).

**Fig.12.** Soccer plots for simulated regional rural fine  $SO_4$  (a,d),  $NO_3$  (b,e) and  $NH_4$  (c,f) levels over Europe (upper panel) and North America (lower panel).

**Fig.13.** Soccer (a,b) and diurnal time series (c,d) plots for observed and simulated AOD555 over Europe (a,c) and North America (b,d).



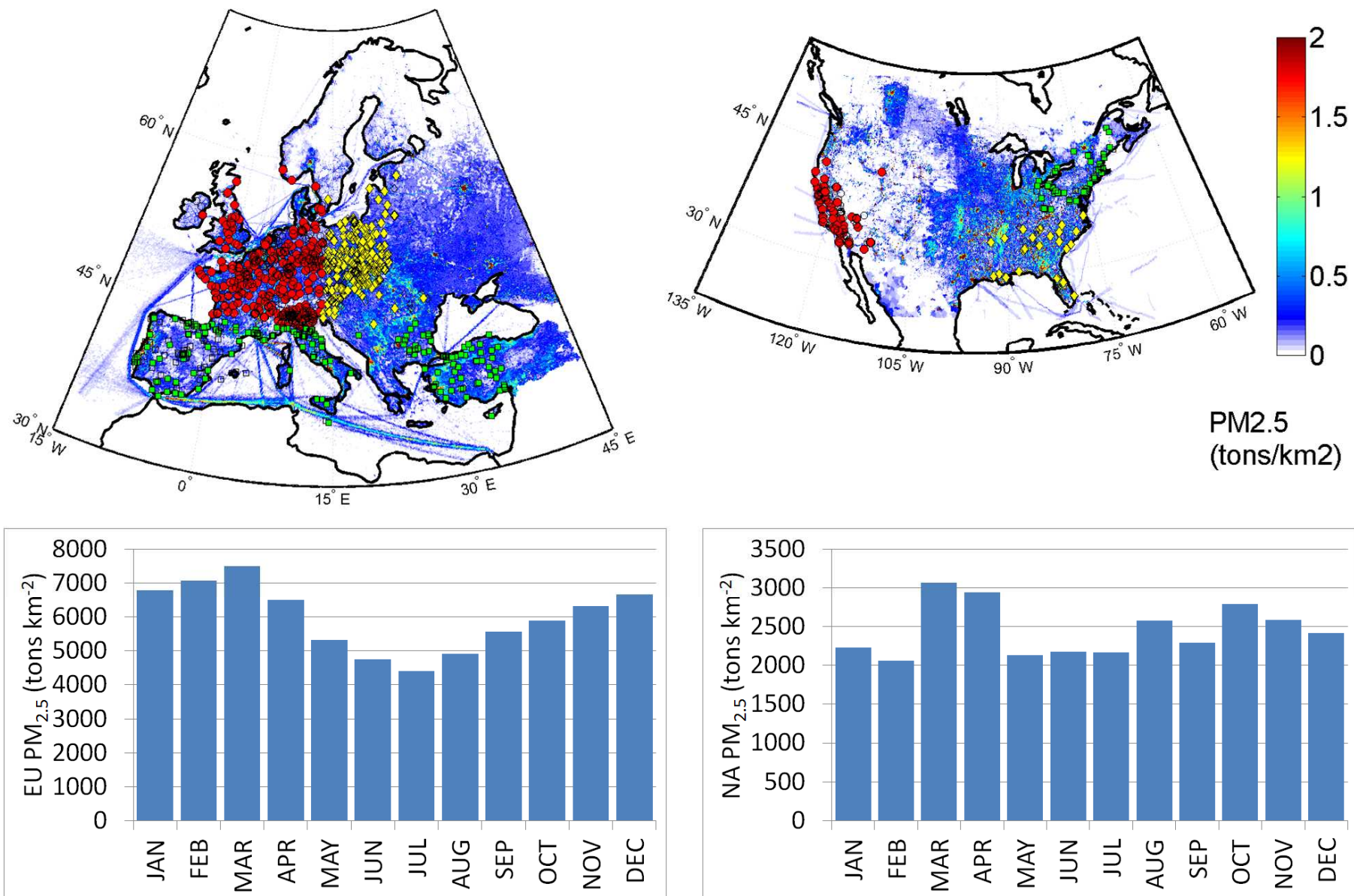


Fig.1

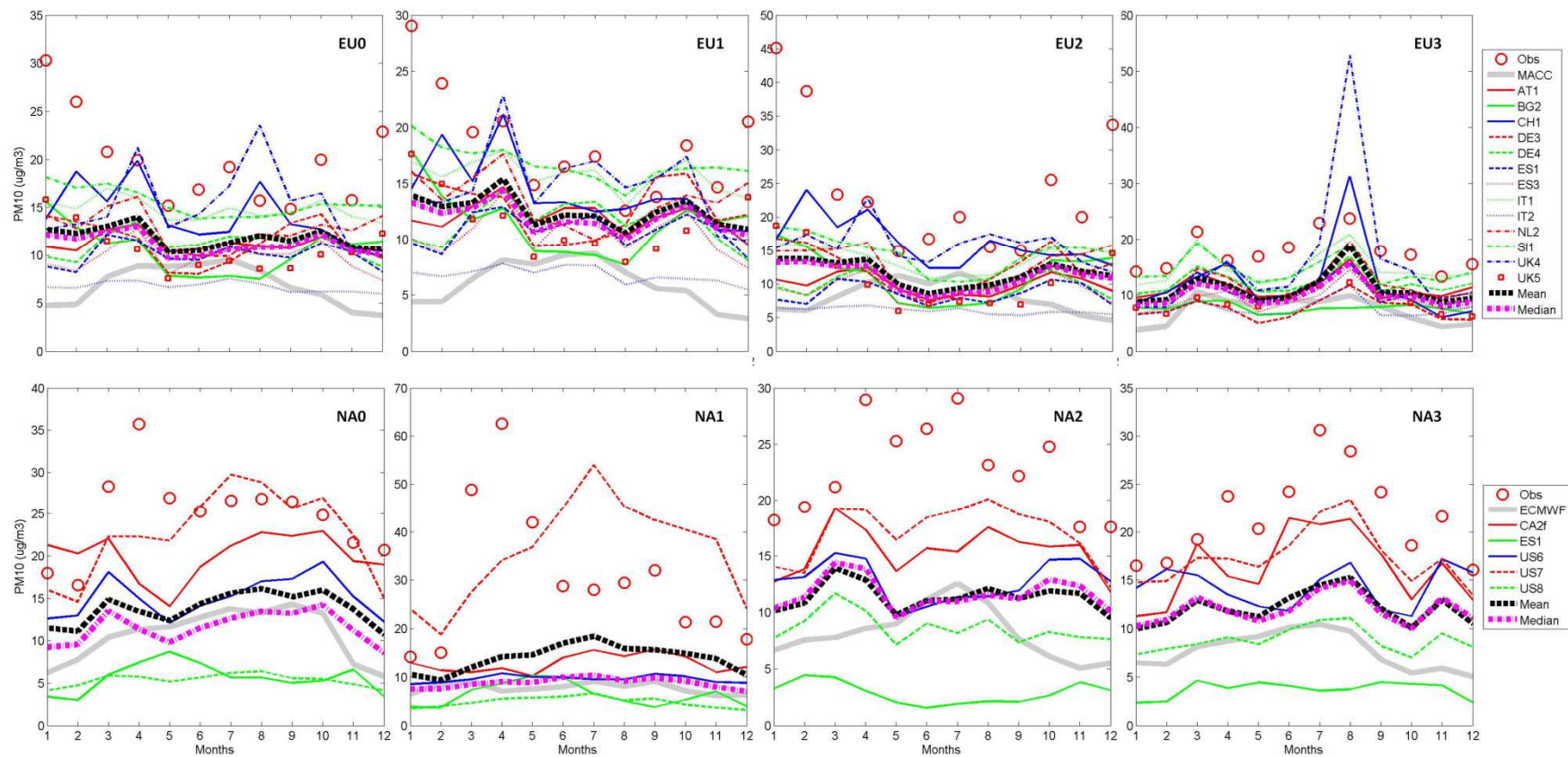


Fig.2

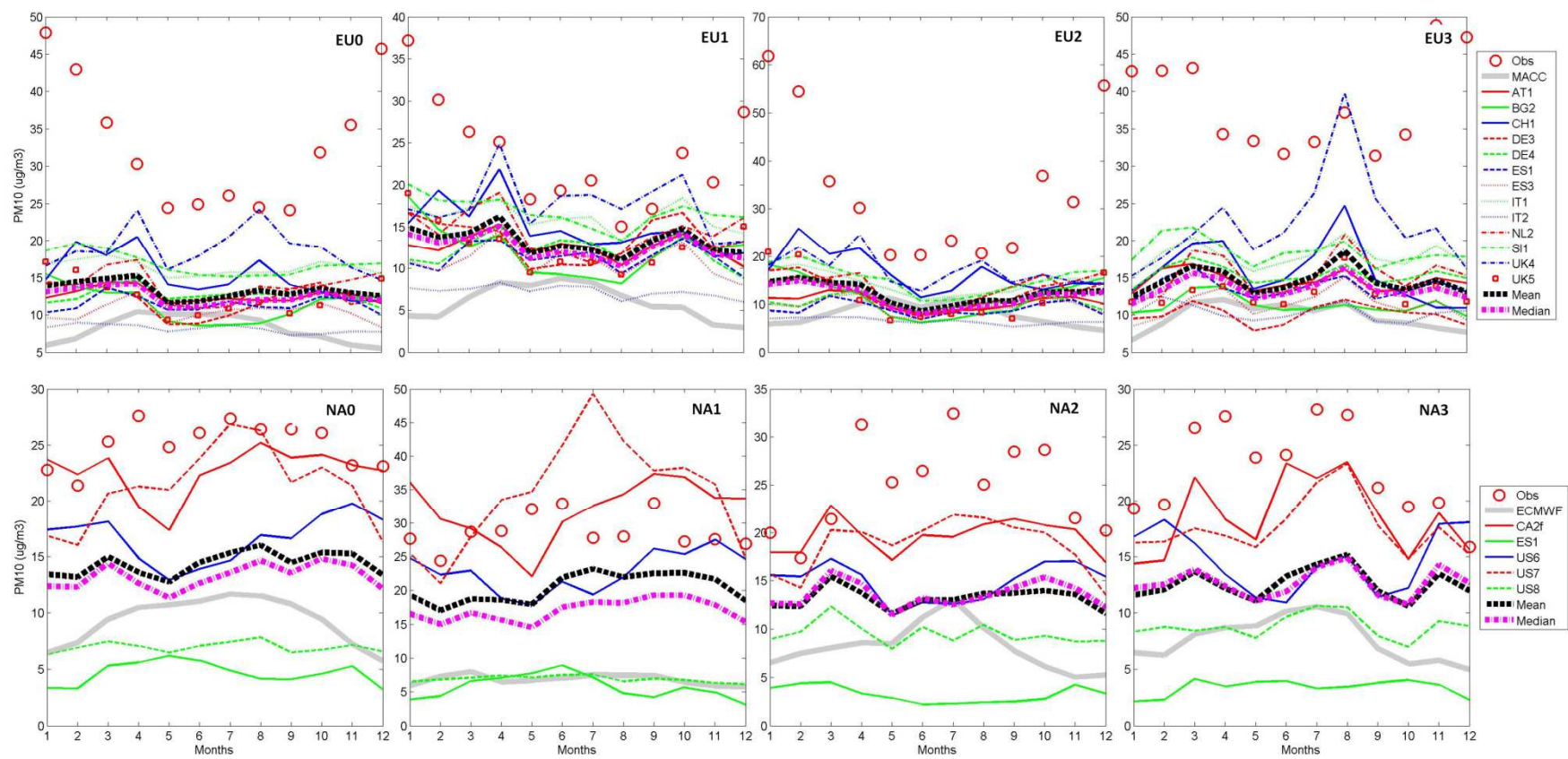


Fig.3



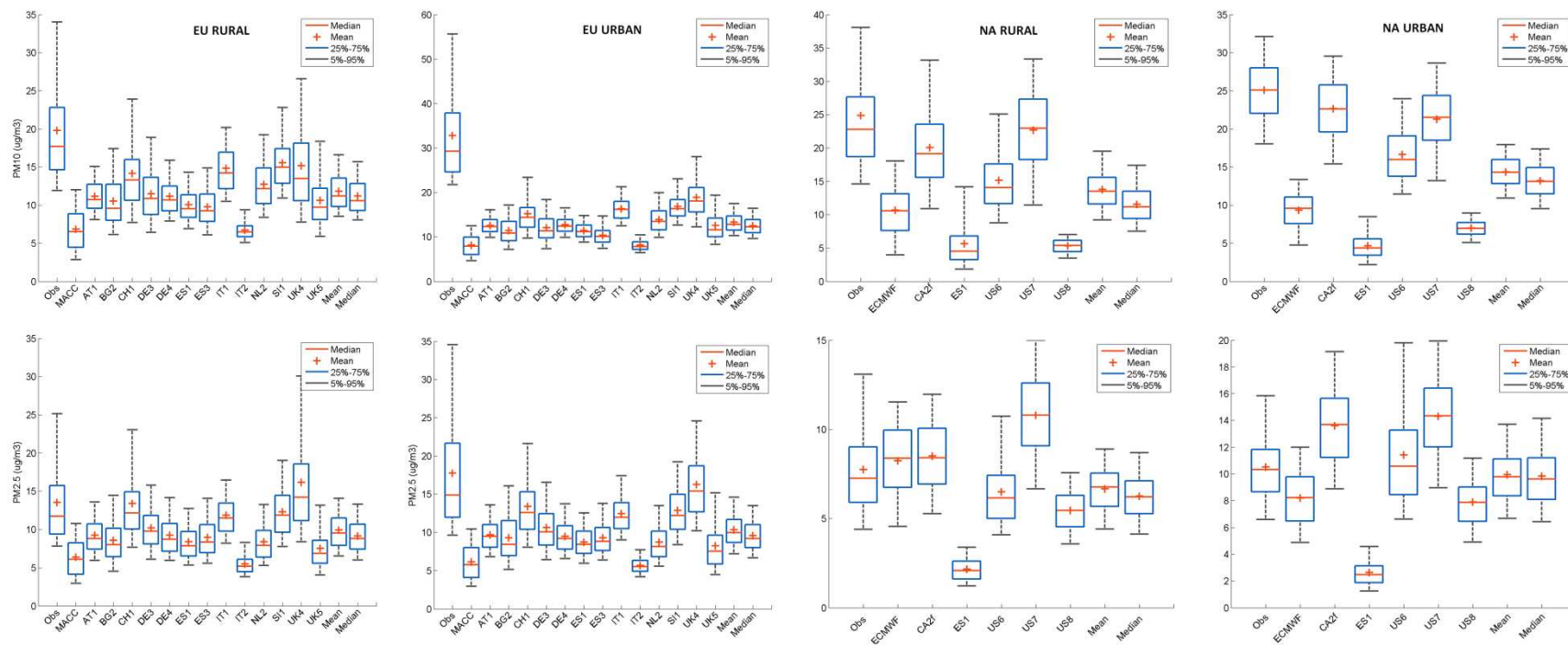


Fig.4

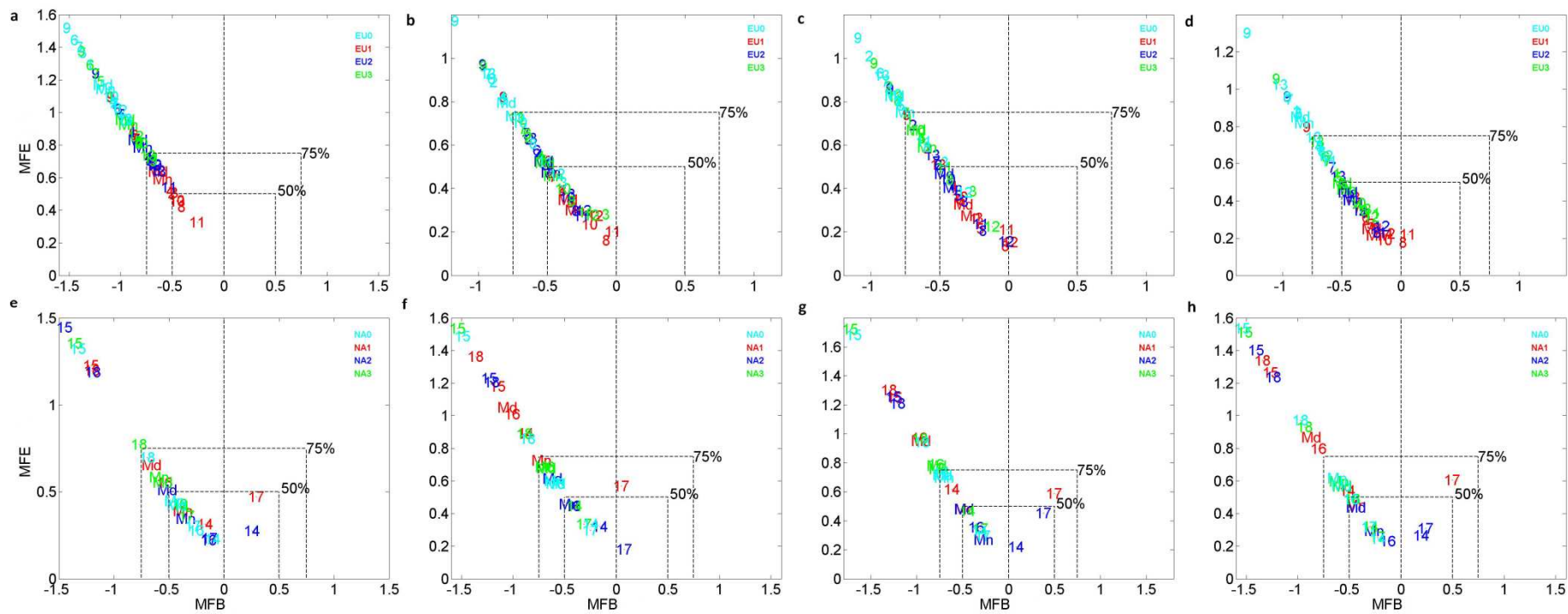


Fig.5

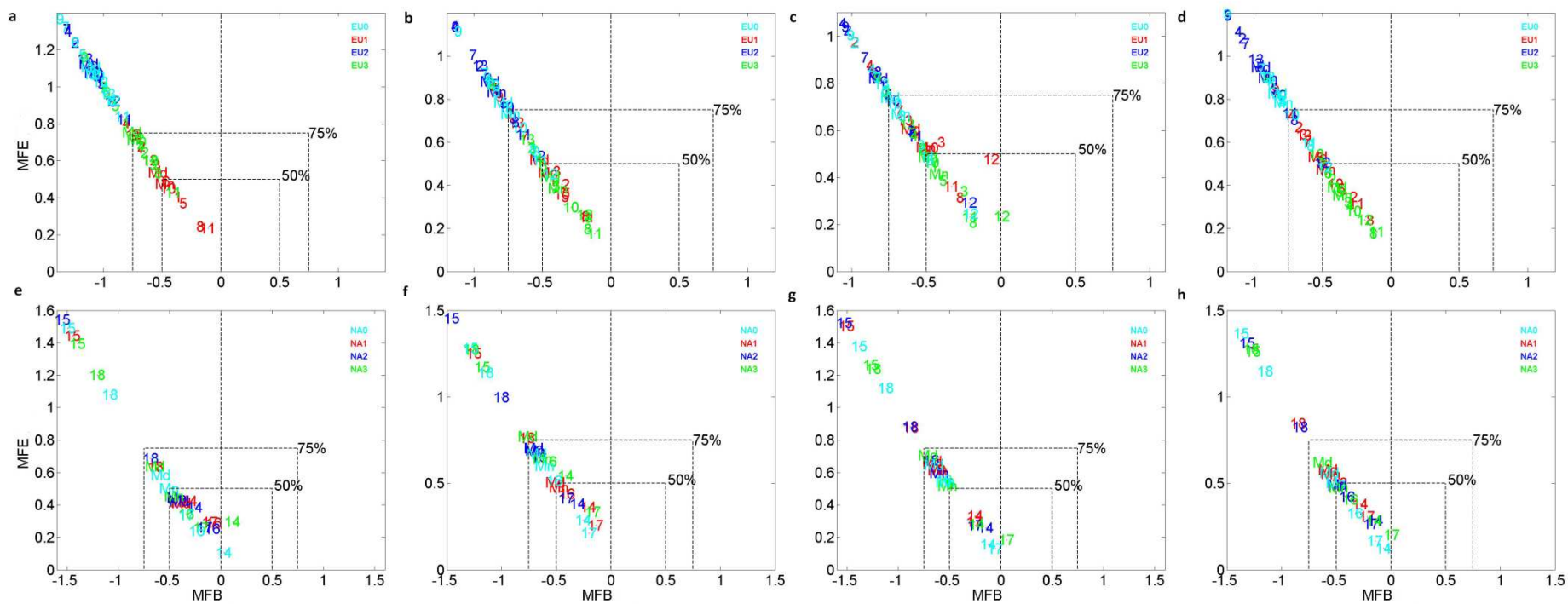


Fig.6



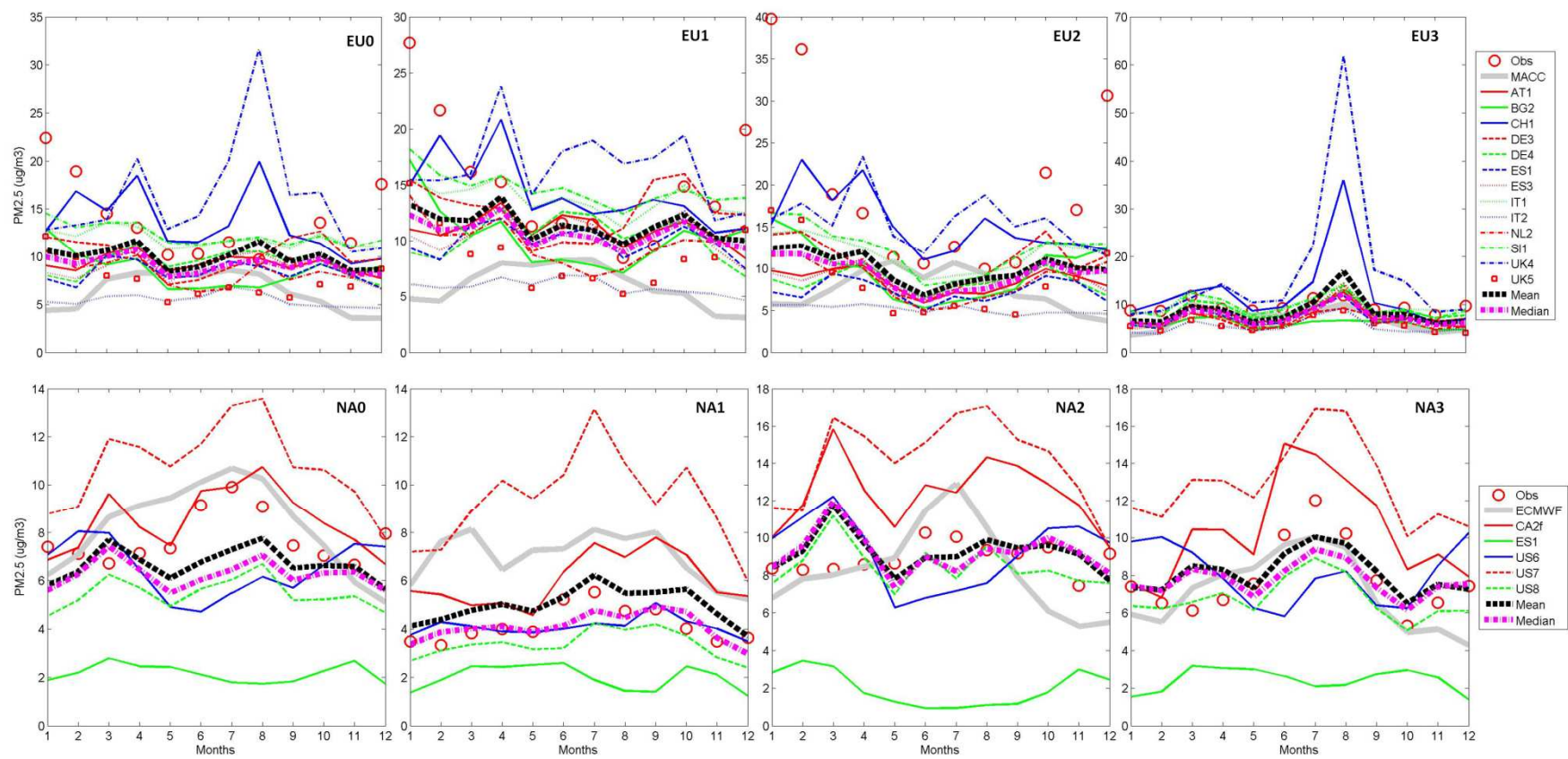


Fig.7

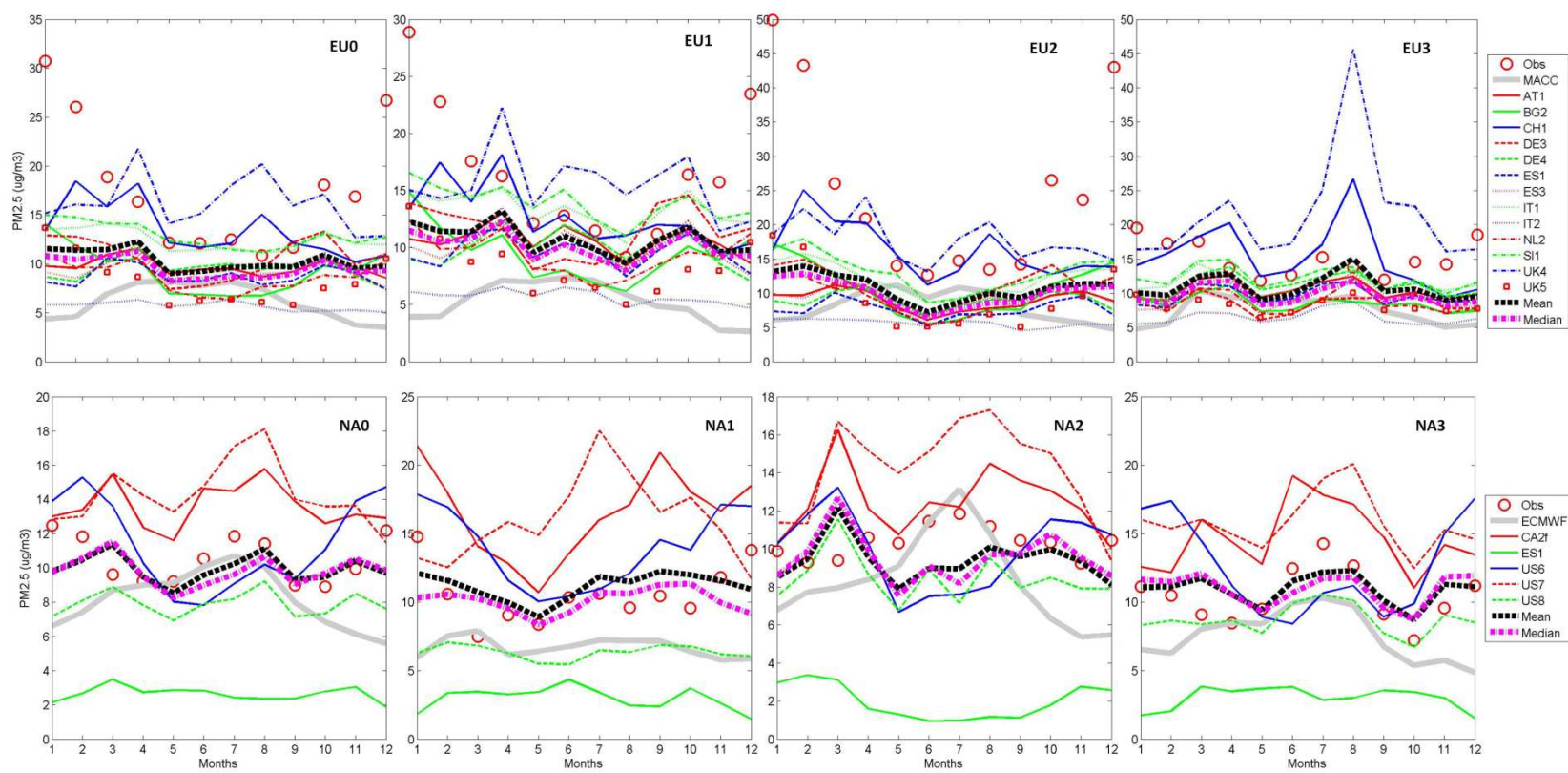


Fig.8

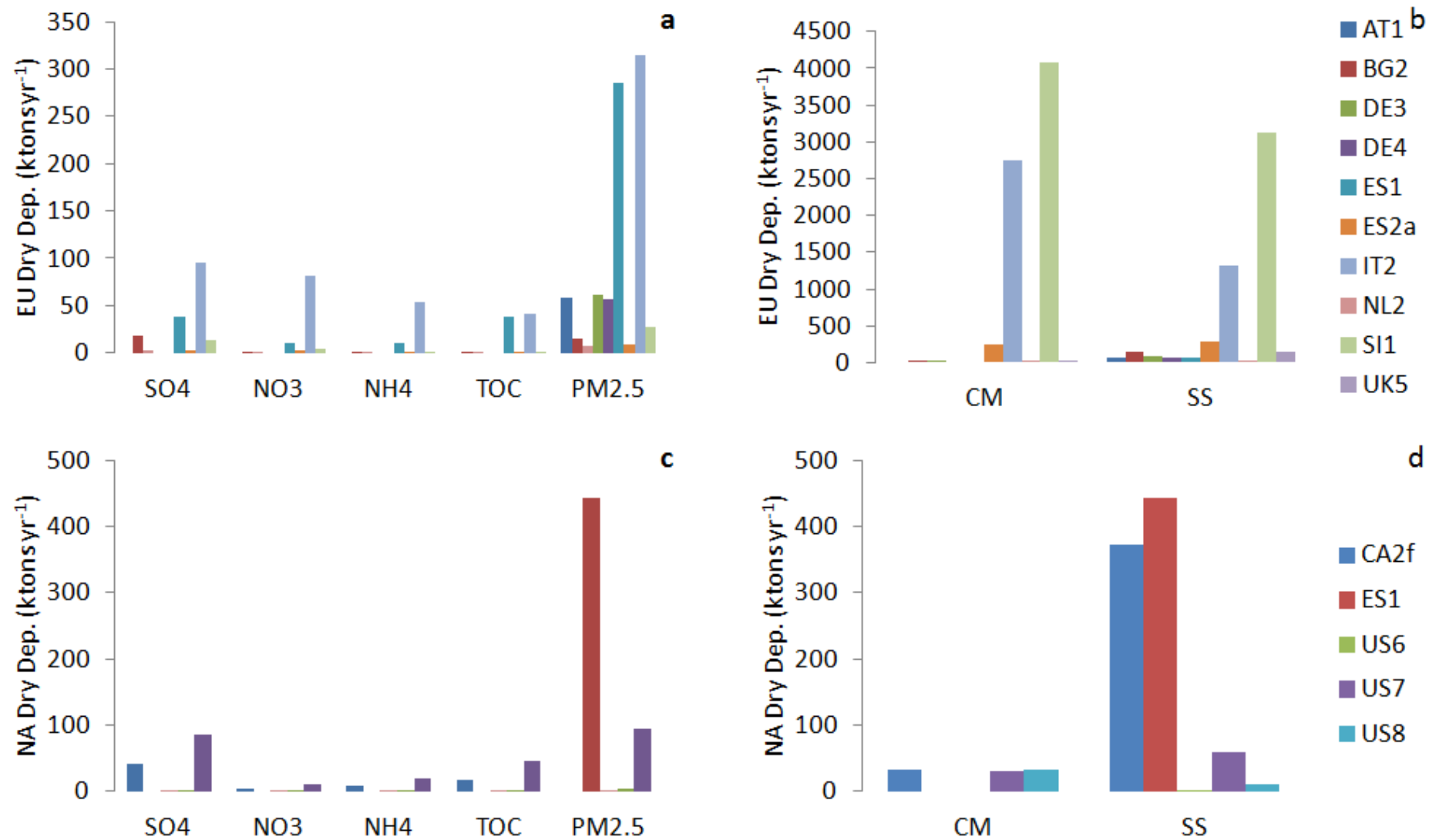


Fig.9

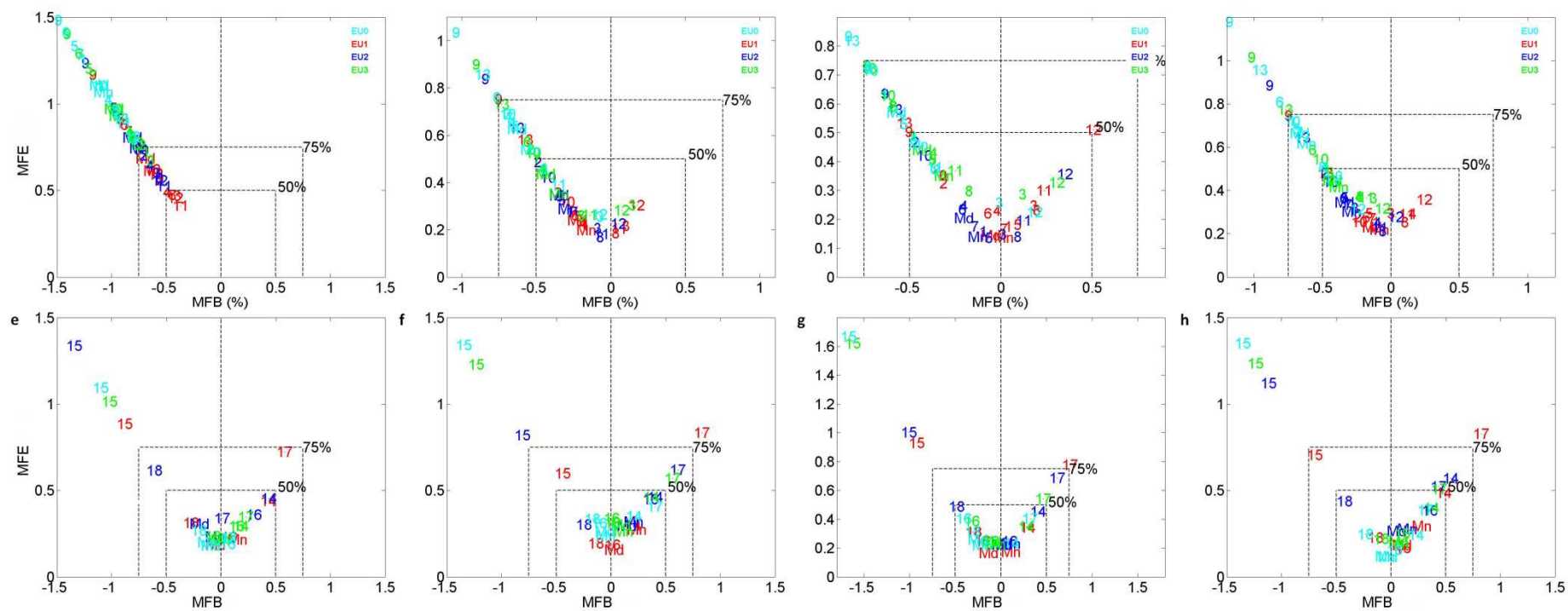


Fig.10

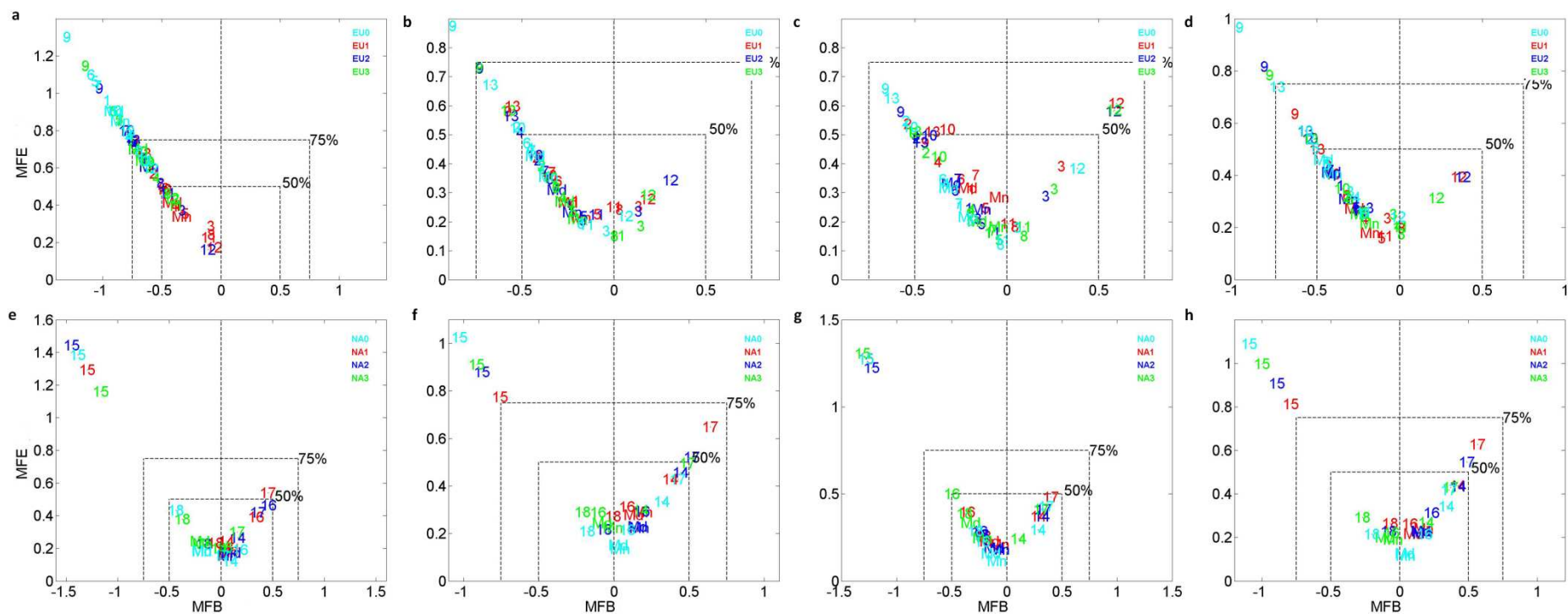


Fig.11



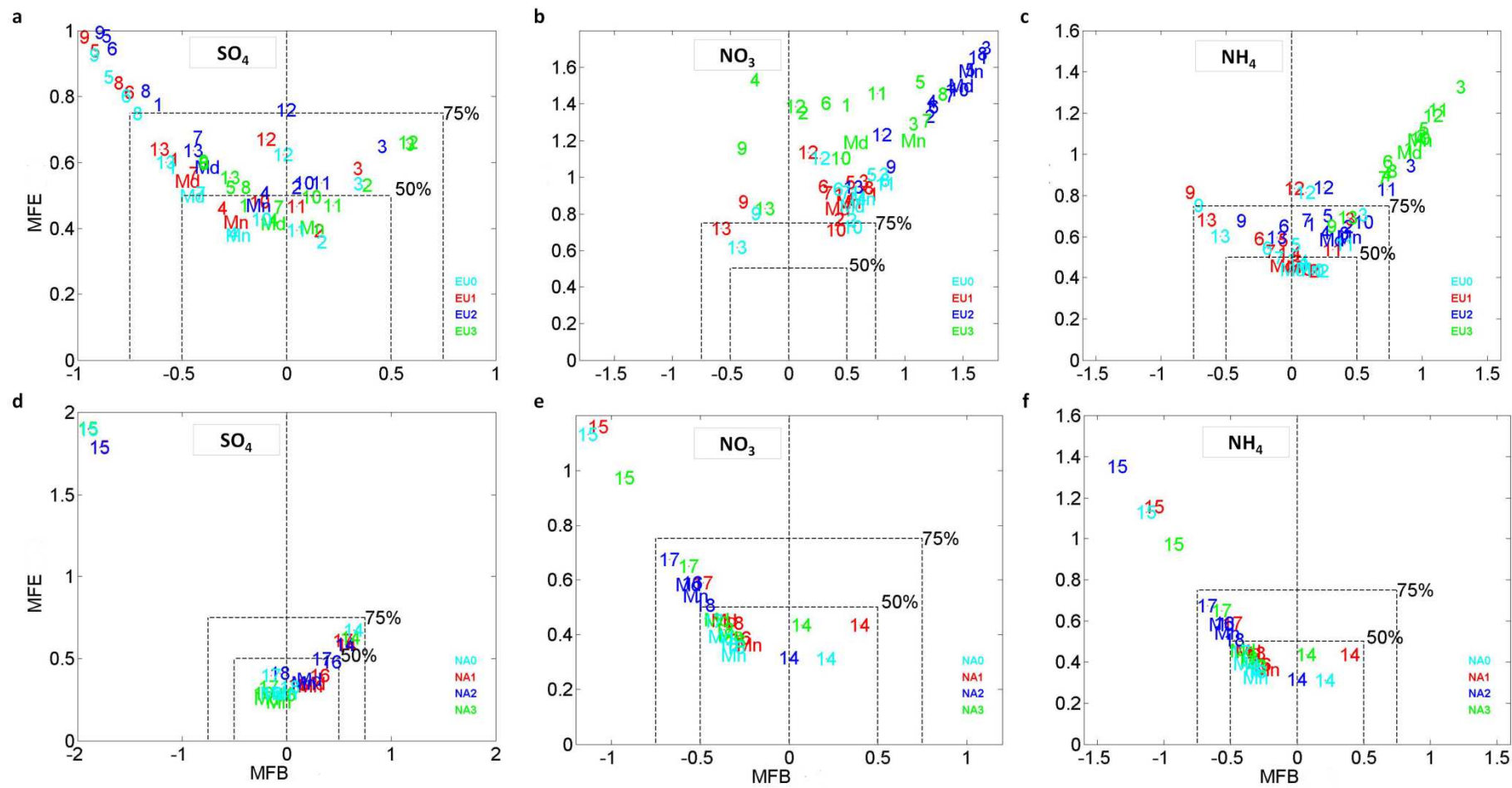


Fig.12

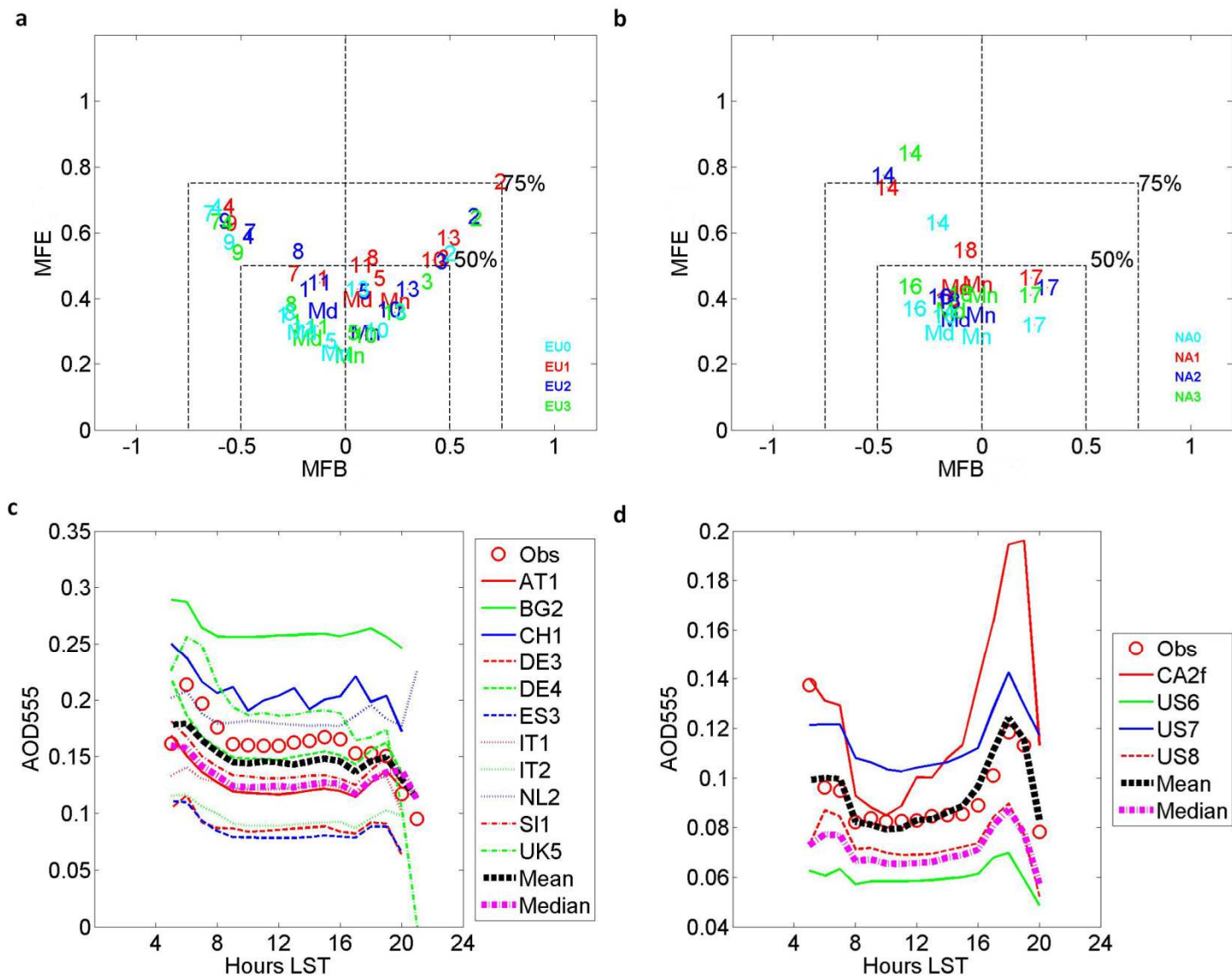


Fig.13

## Supplementary Material

for

### Evaluation of operational online-coupled regional air quality models over Europe and North America in the context of AQMEII phase 2. Part II: Particulate Matter

Ulas Im<sup>a</sup>, Roberto Bianconi<sup>b</sup>, Efsio Solazzo<sup>a</sup>, Ioannis Kioutsioukis<sup>a</sup>, Alba Badia<sup>c</sup>, Alessandra Balzarini<sup>d</sup>, Rocío Baró<sup>e</sup>, Roberto Bellasio<sup>b</sup>, Dominik Brunner<sup>f</sup>, Charles Chemel<sup>g</sup>, Gabriele Curci<sup>h</sup>, Hugo Denier van der Gon<sup>i</sup>, Johannes Flemming<sup>j</sup>, Renate Forkel<sup>k</sup>, Lea Giordano<sup>f</sup>, Pedro Jiménez-Guerrero<sup>e</sup>, Marcus Hirtl<sup>l</sup>, Alma Hodzic<sup>m</sup>, Luka Honzak<sup>n</sup>, Oriol Jorba<sup>c</sup>, Christoph Knote<sup>m</sup>, Paul A. Makar<sup>o</sup>, Astrid Manders-Groot<sup>i</sup>, Lucy Neal<sup>p</sup>, Juan L. Pérez<sup>q</sup>, Guidio Pirovano<sup>d</sup>, George Pouliot<sup>r</sup>, Roberto San Jose<sup>q</sup>, Nicholas Savage<sup>p</sup>, Wolfram Schroder<sup>s</sup>, Ranjeet S. Sokhi<sup>g</sup>, Dimiter Syrakov<sup>t</sup>, Alfreida Torian<sup>r</sup>, Paolo Tuccella<sup>h</sup>, Kai Wang<sup>u</sup>, Johannes Werhahn<sup>k</sup>, Ralf Wolke<sup>s</sup>, Rahela Zabkar<sup>n,v</sup>, Yang Zhang<sup>u</sup>, Junhua Zhang<sup>o</sup>, Christian Hogrefe<sup>r</sup>, Stefano Galmarini<sup>a\*</sup>

- a. European Commission, Joint Research Centre, Institute for Environment and Sustainability, Air and Climate Unit, Ispra (Italy).
- b. Enviroware srl, Concorezzo (MB), Italy.
- c. Earth Sciences Department, Barcelona Supercomputing Center (BSC-CNS), Barcelona, Spain.
- d. Ricerca sul Sistema Energetico (RSE SpA), Milano, Italy
- e. University of Murcia, Department of Physics, Physics of the Earth. Campus de Espinardo, Ed. CIOyN, 30100 Murcia, Spain.
- f. Laboratory for Air Pollution and Environmental Technology, Empa, Dubendorf, Switzerland.
- g. Centre for Atmospheric & Instrumentation Research, University of Hertfordshire, College Lane, Hatfield, AL10 9AB, UK.
- h. Department of Physical and Chemical Sciences, Center of Excellence for the forecast of Severe Weather (CETEMPS), University of L'Aquila, L'Aquila, Italy.
- i. Netherlands Organization for Applied Scientific Research (TNO), Utrecht, The Netherlands.
- j. ECMWF, Shinfield Park, RG2 9AX Reading, United Kingdom.
- k. Karlsruher Institut für Technologie (KIT), Institut für Meteorologie und Klimaforschung, Atmosphärische Umweltforschung (IMK-IFU), Kreuzeckbahnstr. 19, 82467 Garmisch-Partenkirchen, Germany.
- l. Section Environmental Meteorology, Division Customer Service, ZAMG - Zentralanstalt für Meteorologie und Geodynamik, 1190 Wien, Austria.
- m. National Center for Atmospheric Research, Boulder, CO, US.
- n. Center of Excellence SPACE-SI, Ljubljana, Slovenia.
- o. Air Quality Research Section, Atmospheric Science and Technology Directorate, Environment Canada, 4905 Dufferin Street, Toronto, Ontario, Canada.
- p. Met Office, FitzRoy Road, Exeter, EX1 3PB, United Kingdom.

- q. Environmental Software and Modelling Group, Computer Science School - Technical University of Madrid, Campus de Montegancedo - Boadilla del Monte-28660, Madrid, Spain.
- r. Emissions and Model Evaluation Branch, Atmospheric Modeling and Analysis Division/NERL/ORD, Research Triangle Park, North Carolina, USA.
- s. Leibniz Institute for Tropospheric Research, Permoserstr. 15, D-04318 Leipzig, Germany.
- t. National Institute of Meteorology and Hydrology, Bulgarian Academy of Sciences, 66 Tzarigradsko shaussee Blvd., Sofia 1784, Bulgaria.
- u. Department of Marine, Earth and Atmospheric Sciences, North Carolina State University, Raleigh, USA.
- v. University of Ljubljana, Faculty of Mathematics and Physics, Ljubljana, Slovenia.

\* Corresponding author: S. Galmarini ([Stefano.galmarini@jrc.ec.europa.eu](mailto:Stefano.galmarini@jrc.ec.europa.eu))

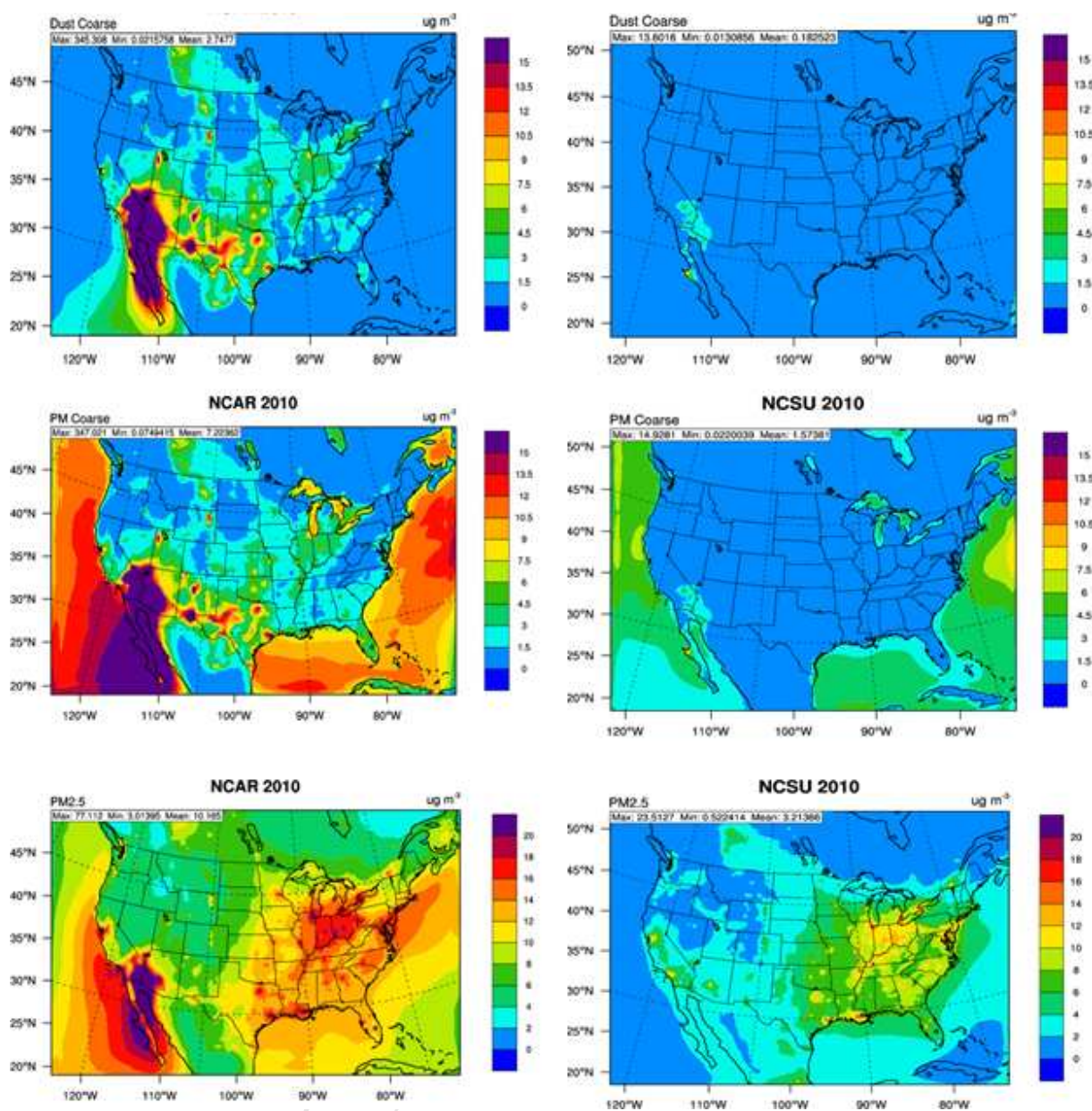


Fig.S1. Simulated concentrations of coarse dust, coarse PM, and fine PM by US7 and US8 over the North America domain for 2010.